

MicroRNA-33 Deficiency Reduces the Progression of Atherosclerotic Plaque in ApoE^{-/-} Mice

Takahiro Horie, MD, PhD; Osamu Baba, MD; Yasuhide Kuwabara, MD, PhD; Yoshimasa Chujo, MD; Shin Watanabe, MD, PhD; Minako Kinoshita, MD, PhD; Masahito Horiguchi, MD, PhD; Tomoyuki Nakamura, MD, PhD; Kazuhisa Chonabayashi, MD, PhD; Masakatsu Hishizawa, MD, PhD; Koji Hasegawa, MD, PhD; Noriaki Kume, MD, PhD; Masayuki Yokode, MD, PhD; Toru Kita, MD, PhD; Takeshi Kimura, MD, PhD; Koh Ono, MD, PhD

Background—Cholesterol efflux from cells to apolipoprotein A-I (apoA-I) acceptors via the ATP-binding cassette transporters ABCA1 and ABCG1 is thought to be central in the antiatherogenic mechanism. MicroRNA (miR)-33 is known to target ABCA1 and ABCG1 in vivo.

Methods and Results—We assessed the impact of the genetic loss of miR-33 in a mouse model of atherosclerosis. MiR-33 and apoE double-knockout mice (miR-33^{-/-}ApoE^{-/-}) showed an increase in circulating HDL-C levels with enhanced cholesterol efflux capacity compared with miR-33^{+/+}ApoE^{-/-} mice. Peritoneal macrophages from miR-33^{-/-}ApoE^{-/-} mice showed enhanced cholesterol efflux to apoA-I and HDL-C compared with miR-33^{+/+}ApoE^{-/-} macrophages. Consistent with these results, miR-33^{-/-}ApoE^{-/-} mice showed reductions in plaque size and lipid content. To elucidate the roles of miR-33 in blood cells, bone marrow transplantation was performed in these mice. Mice transplanted with miR-33^{-/-}ApoE^{-/-} bone marrow showed a significant reduction in lipid content in atherosclerotic plaque compared with mice transplanted with miR-33^{+/+}ApoE^{-/-} bone marrow, without an elevation of HDL-C. Some of the validated targets of miR-33 such as RIP140 (NR1P1) and CROT were upregulated in miR-33^{-/-}ApoE^{-/-} mice compared with miR-33^{+/+}ApoE^{-/-} mice, whereas CPT1a and AMPK α were not.

Conclusions—These data demonstrate that miR-33 deficiency serves to raise HDL-C, increase cholesterol efflux from macrophages via ABCA1 and ABCG1, and prevent the progression of atherosclerosis. Many genes are altered in miR-33-deficient mice, and detailed experiments are required to establish miR-33 targeting therapy in humans. (*J Am Heart Assoc.* 2012;1:e003376 doi: 10.1161/JAHA.112.003376)

Key Words: ABCA1 • ABCG1 • atherosclerosis • HDL-C • microRNA

Although the lowering of LDL cholesterol (LDL-C) with the use of statins has revolutionized the treatment of atherosclerotic cardiovascular disease, statins can only

reduce the risk of cardiovascular events by up to 50% depending on the disease status and the amount of statin used, which still leaves a large burden of residual disease risk.¹⁻³ Recent studies have shown that HDL cholesterol (HDL-C) levels under statin treatment remain an independent predictor of the risk of cardiovascular events in patients who have been treated with statins to lower LDL-C levels⁴ and that HDL-C levels at baseline are a strong predictor of 12-month morbidity and mortality from cardiovascular events in patients on statins with low LDL-C levels undergoing stent placement for acute coronary syndromes.⁵ Thus, clinical and epidemiological studies have consistently shown that there is an inverse relationship between HDL-C concentration and cardiovascular risk. In fact, a 1 mg/dL (0.026 mmol/L) increment in HDL-C levels was associated with a significant decrease in the risk of coronary heart disease of 2% in men and 3% in women.⁶ All these data led us to the idea that the development of therapies that raise HDL-C is necessary to reduce cardiovascular diseases in the midst of the “statin era” in the management of atherosclerosis. Transgenic mice that

From the Departments of Cardiovascular Medicine (T.H., O.B., Y.K., Y.C., S.W., M.K., M. Horiguchi, N.K., T. Kimura, K.O.), Hematology and Oncology (K.C., M. Hishizawa), and Clinical Innovative Medicine, Translational Research Center (T.H., M.Y.), Graduate School of Medicine, Kyoto University, Kyoto, Japan; Department of Pharmacology, Kansai Medical University, Moriguchi, Osaka, Japan (T.N.); Division of Translational Research, Clinical Research Institute, Kyoto Medical Center, Kyoto, Japan (K.H.); Department of Cardiovascular Medicine, Kobe City Medical Center General Hospital, Kobe, Japan (T. Kita).

Drs Horie and Baba contributed equally to this article.

Correspondence to: Koh Ono, MD, PhD, Department of Cardiovascular Medicine, Graduate School of Medicine, Kyoto University, Kyoto, 54 Shogoinkawahara-cho, Sakyo-ku, Kyoto, 606-8507, Japan. E-mail: kohono@kuhp.kyoto-u.ac.jp

Received August 14, 2012; accepted September 28, 2012.

© 2012 The Authors. Published on behalf of the American Heart Association, Inc., by Wiley-Blackwell. This is an Open Access article under the terms of the Creative Commons Attribution Noncommercial License, which permits use, distribution, and reproduction in any medium, provided the original work is properly cited and is not used for commercial purposes.

overexpress apoA-I and the infusion of apoA-I/phospholipid complexes in humans are associated with reduced progression or regression of atherosclerosis.^{7–9} These observations have suggested that HDL-C-raising therapies might be an effective way to reduce the residual risk of cardiovascular diseases in patients who are being treated with current therapies.

The identification of ATP-binding cassette transporter A1 (ABCA1) as a rate-limiting factor in HDL-C biogenesis suggested that increased ABCA1 activity could inhibit atherosclerosis. Studies in mice in which the *Abca1* locus is either deleted or overexpressed generally have supported the hypothesis that ABCA1 significantly prevents atherosclerosis by maintaining circulating HDL-C levels and cellular cholesterol efflux.^{10–13} Tissue-specific knockouts of the *Abca1* locus were generated and revealed that liver and macrophage ABCA1 both play roles in preventing atherosclerosis.¹⁴ ABCA1 modulates cell-surface cholesterol levels, inhibits its partitioning into lipid rafts, and decreases the responsiveness of inflammatory signals from innate immune receptors. Moreover, ABCA1 has been reported to act directly as an anti-inflammatory receptor independent of its lipid transport activities.¹⁵ Therefore, augmentation of the function of ABCA1 might be a beneficial therapeutic approach.

MicroRNA (miR) is small, nonprotein-coding RNA that binds to specific mRNA and inhibits translation or promotes mRNA degradation. Recent reports, including ours, have indicated that miR-33 controls cholesterol homeostasis based on knockdown experiments using antisense technology.^{16–18} Moreover, antisense inhibition of miR-33 resulted in a regression of the atherosclerotic plaque volume in LDL-receptor-deficient mice.¹⁹ Antisense inhibition of miRNA function is an important tool for elucidating miRNA biology and evaluating its therapeutic potential. However, to determine the organ-/cell-type-specific function of miRNA over the long term in vivo, studies on miRNA-deficient mice and the analysis of specific organ/cell types from these mice are needed, especially for the development of therapeutic strategies for chronic diseases, such as atherosclerosis, dyslipidemia, and metabolic syndrome.

In the present study, we crossed miR-33-deficient mice (miR-33^{-/-}) with apoE-deficient mice (*ApoE*^{-/-}) to examine the impact of miR-33 deletion on the progression of atherosclerosis and demonstrated that genetic loss of miR-33 raises circulating HDL-C and decreases atherosclerotic plaque size. Furthermore, loss of leukocyte miR-33 significantly reduced the lipid content in atherosclerotic plaque. Our results indicate that miR-33 deficiency raises both HDL-C and macrophage cholesterol efflux and strongly suggest that miR-33 should be considered as a potential target for the prevention of atherosclerosis. However, some of the previously validated targets of miR-33, such as RIP140 and CROT,

were upregulated in miR-33^{-/-}*ApoE*^{-/-} mice compared with miR-33^{+/+}*ApoE*^{-/-} mice, whereas CPT1a and AMPK α were not. Moreover, the effect of miR-33 deletion in macrophages is not as simple as the shift from the M1 to M2 phenotype reported previously.¹⁹ Thus, to establish that the silencing of miRNA is a therapeutic strategy for the treatment of humans, further detailed experiments are required.

Methods

Cell Culture and Reagents

Peritoneal macrophages were obtained from the peritoneal cavity of mice 4 days after intraperitoneal injection of 3 mL of 3% thioglycollate. For the analysis of M1/M2 markers, residual peritoneal macrophages were obtained without thioglycollate injection. The cells obtained were washed, spun at 1000 rpm for 5 minutes, and plated at a density of 5×10^5 cells/mL with RPMI1640 medium (Nacalai Tesque, Japan) containing 10% fetal bovine serum (FBS). J774 mouse macrophages were obtained from the American Type Cell Collection (Rockville, MD) and cultured with RPMI1640 medium containing 10% FBS. The antibodies used were an anti-ABCA1 antibody (NB400-105), an anti-ABCG1 antibody (NB400-132; Novus Biologicals, Littleton, CO), an anti-GAPDH antibody (#2118S), an anti-AMPK α antibody (#2532), an anti-cleaved-caspase-3 antibody (#9661S; Cell Signaling Technology, Beverly, MA), an anti- β -actin antibody (AC-15; A5441, Sigma-Aldrich, St. Louis, MO), an anti-RIP140 antibody (sc-8997), an anti-CD3 ϵ antibody (sc-1127; Santa Cruz, Biotechnology, CA), an anti- α SMA antibody (MO0851, Dako, Glostrup, Denmark), an anti-CROT antibody (ab103448), an anti-CPT1A antibody (ab128568), an anti-iNOS antibody (ab3523), an anti-VCAM1 antibody (ab27560), an anti-ICAM1 antibody (ab25375), an anti-IL6 antibody (ab6672), an anti-IL10 antibody (ab33471; Abcam, Cambridge, UK), an anti-single-stranded DNA (ssDNA) antibody (No. 18731; IBL, Gunma, Japan), and an anti-CD68 antibody (FA-11; Serotec, Kidlington, UK). Human acetylated LDL (acLDL) and human HDL-C were purchased from Biomedical Technologies Inc (Stoughton, MA). Anti-rabbit and anti-mouse IgG HRP-linked antibody was purchased from GE Healthcare (Amersham, UK). Human apoA-I, polyethylene glycol (PEG), ACAT inhibitor, Cpt-cAMP, Sudan IV, and oil red O were from Sigma-Aldrich. [1, 2-³H]-Cholesterol was from Perkin Elmer (Boston, MA).

Generation of MiR-33 and ApoE Double-Knockout Mice

To obtain miR-33 and apoE double-knockout mice (miR-33^{-/-}*ApoE*^{-/-}), miR-33^{-/-} mice were mated with *ApoE*^{-/-} mice, which were backcrossed to C57BL/6 mice for 10 generations.^{20–22} Because both knockout mice had a BL/6 background,

miR-33^{-/-}*ApoE*^{-/-} mice also had a BL/6 background. MiR-33^{+/+}*ApoE*^{-/-} littermates were used as controls. After being weaned at 4 weeks of age, mice were fed normal chow (NC) containing 4.5% fat (Oriental Yeast, Tokyo, Japan) until 6 weeks of age and then switched to a Western-type diet (WTD) containing 0.15% cholesterol and 20% fat (Oriental Yeast) for 16 weeks. All the experimental protocols were approved by the Ethics Committee for Animal Experiments of Kyoto University.

Serum Lipid Profiling

After mice were fasted for 4 to 6 hours, blood was obtained from the inferior vena cava of anesthetized mice, and serum was separated by centrifugation at 4°C and stored at -80°C. Serum lipoproteins were measured by standard methods (Accelerator selective detergent method using a Hitachi 7180 Auto Analyzer; Nagahama Life Science Laboratory, Nagahama, Japan) and HPLC methods (Sky Light Biotech, Akita, Japan).

Western Blotting

Western blotting was performed using standard procedures as described previously.²³ A total of 20 μg of protein was fractionated using NuPAGE 4% to 12% Bis-Tris gels (Invitrogen) and transferred to a Protran nitrocellulose transfer membrane (Whatman). The membrane was blocked using 1× phosphate-buffered saline (PBS) containing 5% nonfat milk for 1 hour and incubated with the primary antibody (anti-ABCA1, 1:1000; anti-ABCG1, 1:1000; anti-cleaved caspase-3, 1:500; anti-AMPKα, 1:1000; anti-CROT, 1:100; anti-CPT1a, 1:1000; anti-RIP140, 1:500; anti-β-actin, 1:3000; anti-GAPDH, 1:3000) overnight at 4°C. Following a washing step in PBS-0.05% Tween 20 (0.05% T-PBS), the membrane was incubated with the secondary antibody (anti-rabbit or anti-mouse IgG HRP-linked, 1:2000) for 1 hour at 4°C. The membrane was then washed in 0.05% T-PBS and detected by ECL Western Blotting Detection Reagent (GE Healthcare) using an LAS-1000 system (Fuji Film).

RNA Extraction and Quantitative Real-Time PCR (qRT-PCR)

Total RNA was isolated and purified using TRIzol reagent (Invitrogen), and cDNA was synthesized from 1 μg of total RNA using Transcriptor First Strand cDNA Synthesis Kit (Roche) in accordance with the manufacturer's instructions. For qRT-PCR, specific genes were amplified by 40 cycles using SYBR Green PCR Master Mix (Applied Biosystems). Expression was normalized to the housekeeping gene *Actb*. Gene-specific primers are summarized as follows:

Irf6 sense, 5' ACCACGGCCTTCCCTACTTC 3';
Irf6 antisense, 5' AGATTGTTTTCTGCAAGTGCATCA 3';
Tnf sense, 5' CCAGACCCTCACACTCAGATC 3';

Tnf antisense, 5' CACTTGGTGGTTTGTACGAC 3';
Nos2 (*Inos*) sense, 5' GAGTCTTGGTAAAGTGGTGTC 3';
Nos2 (*Inos*) antisense, 5' TTCCCTGTCTCAGTAGCAAAGAG 3';
Mmp2 sense, 5' ATCTTTCAGGAGACAAGTTCTG 3';
Mmp2 antisense, 5' TTCAGGTAATAAGCACCTTGAA 3';
Serpine 1 (*Pai1*) sense, 5' TCAGCCCTTGCTTGCCTCAT 3';
Serpine 1 (*Pai1*) antisense, 5' GCATAGCCAGCACCGAGGA 3';
Il10 sense, 5' AAATAAGAGCAAGGCAGTGGAG 3';
Il10 antisense, 5' TCATTCATGGCCTTGTAGACAC 3';
Arg1 sense, 5' AACTCTTGGGAAGACAGCAGAG 3';
Arg1 antisense, 5' GTAGTCAGTCCCTGGCTTATGG 3';
Retnla (*Fizz1*) sense, 5' AGGATGCCAACTTTGAATAGGA 3';
Retnla (*Fizz1*) antisense, 5' AGTTAGCTGGATTGGCAAGAAG 3';
Chi3l3 (*Ym-1*) sense, 5' CCCACCAGGAAAGTACACAGA 3';
Chi3l3 (*Ym-1*) antisense, 5' CTCAGTGGCTCCTTCAATCAG 3';
Emr1 (*F4/80*) sense, 5' TCCAGAAGGCTCCCAAGGATA 3';
Emr1 (*F4/80*) antisense, 5' GGGCACTTTTGTCTCACAGGTA 3';
Abca1 sense, 5' AACAGTTTGTGGCCCTTTTG 3';
Abca1 antisense, 5' AGTTCAGGCTGGGGTACTT 3';
Abcg1 sense, 5' CTGCCTCACCTCACTGTTC 3';
Abcg1 antisense, 5' TCTCGTCTGCCTTCATCCTT 3';
Crot sense, 5' TACTTTTACCACGGCCGAAC 3';
Crot antisense, 5' GACGGTCAAATCCTTTTCCA 3';
Cpt1a sense, 5' GATCTACAATCCCCTCTGCTCT 3';
Cpt1a antisense, 5' TAGAGCCAGACCTTGAAGTAAAG 3';
Prkaa1 (*AMPKα1*) sense, 5' AGAGGGCCGCAATAAAAGAT 3';
Prkaa1 (*AMPKα1*) antisense, 5' TGTGTACAGGCAGCTGAGG 3';
Nrip1 (*RIP140*) sense, 5' AGCAGGACAAGAGTCACAGAAAC 3';
Nrip1 (*RIP140*) antisense, 5' TGTGATGATTGGCAGTATCTACG 3';
Actb sense, 5' GATCTGGCACCACACCTTCT 3';
Actb antisense, 5' GGGGTGTTGAAGGTCTCAAA 3';

Quantitative PCR for MicroRNA

Total RNA was isolated using TRIzol reagent (Invitrogen). MiR-33 was measured in accordance with the TaqMan MicroRNA Assays (Applied Biosystems) protocol, and the products were analyzed using a thermal cycler (ABI Prism7900HT sequence detection system). Samples were normalized by U6 snRNA expression.

Cholesterol Efflux via Mouse ApoB-Depleted Serum

Cholesterol efflux via mouse apoB-depleted serum was measured as described previously.^{24,25} Briefly, J774 cells were plated in 24 multiwell plates (7 × 10⁴ cells/well) and labeled for 24 hours using ³H-cholesterol (2 μCi/mL) in RPMI1640 plus 1% FBS. Cells were incubated in RPMI1640 containing Cpt-cAMP (0.3 mmol/L) and 0.2% BSA for an additional 16 hours to upregulate ABCA1 in J774 cells. Cells were washed and incubated for 4 hours in MEM-HEPES

containing 2.8% apoB-depleted serum (equivalent to 2% serum), which was obtained after apoB lipoproteins were removed with PEG.²⁶ All steps were performed in the presence of acyl-coenzyme A:cholesterol acyltransferase (ACAT) inhibitor (2 $\mu\text{g}/\text{mL}$). Cholesterol efflux was expressed as the percentage of radioactivity released from the cells in the medium relative to the total radioactivity in cells plus medium.

Cholesterol Efflux From Mouse Peritoneal Macrophages

Cellular cholesterol efflux via apoA-I and HDL was determined as described previously.^{22,27} Briefly, thioglycollate-elicited mouse peritoneal macrophages were plated in 24-well multiplates at a density of 5×10^6 cell/mL. Cells were cultured for 24 hours in RPMI1640 containing ^3H -labeled acLDL (1.0 $\mu\text{Ci}/\text{mL}$ of ^3H -cholesterol and 25 $\mu\text{g}/\text{mL}$ of acLDL). On the next day, cells were washed 3 times with RPMI1640, then incubated for 6 hours in RPMI1640 with or without apoA-I or HDL as indicated concentrations. Cholesterol efflux was expressed as a percentage of the radioactivity released from cells in medium relative to the total radioactivity in cells plus medium.

Flow Cytometry

Peripheral blood was collected from the orbital sinuses of 12-week-old miR-33^{+/+}*ApoE*^{-/-} and miR-33^{-/-}*ApoE*^{-/-} mice that were given an NC diet using heparin-coated capillary tubes. Total leukocytes were quantified from whole blood using a hematology cell counter (Celltac α MEK-6358, Nihon Kohden). Erythrocytes were lysed using a commercial RBC lysis solution (BD PharmLyse, BD Biosciences). Monocytes were identified by staining with anti-CD115–Alexa Fluor 488 antibody (eBioscience clone AFS98), and monocyte subsets were identified by staining with anti-Ly6C–APC antibody (eBioscience, clone HK1.4). Data were acquired using a BD FACSaria Flow Cytometer and analyzed with BD FACSDiva software (BD Biosciences).

Bone Marrow Transplantation (BMT) and Assessment of Chimerism

Male mice with genotypes of miR-33^{+/+}*ApoE*^{-/-} and miR33^{-/-}*ApoE*^{-/-} (8 weeks old) were used as bone marrow (BM) donors. BM recipients were female miR-33^{+/+}*ApoE*^{-/-} mice and miR-33^{-/-}*ApoE*^{-/-} mice (8 weeks old). Thus, all the experimental mice used for BM transplantation (BMT) had an *ApoE*^{-/-} background. BM donors were euthanized by cervical dislocation, and BM cells were collected by flushing femurs and tibias with PBS supplemented with 3% FBS. The

suspension was passed through 40- μm nylon mesh (Cell Strainer, BD Biosciences). Red blood cells were lysed using ACK lysing buffer (Lonza). BM cells were then washed twice with PBS supplemented with 3% FBS. To induce BM aplasia, recipients were irradiated with 2 doses of 6 Gy within an interval of 3 hours (cesium 137; Gammacell 40 Exactor) and injected intravenously with 5×10^6 BM cells 6 hours after irradiation.^{28,29} After BMT, mice were fed NC diet for 4 weeks and then switched to a WTD for 12 weeks. At age 24 weeks, mice were euthanized and analyzed. The hematologic chimerism of mice was determined by PCR using genomic DNA from blood, BM, and tail with the PCR primers described above and by measuring miR-33 levels in BM cells by quantitative PCR at age 24 weeks (ie, 16 weeks after BMT).

Quantification of Atherosclerosis

Atherosclerotic lesions were quantified by en face analysis of the whole aorta and by cross-sectional analysis of the proximal aorta.^{30–32} For the en face analysis of the aorta, the Sudan IV-stained aortas were photographed and used for the quantification of atherosclerotic lesions. The total aortic surface area and the lesion area were measured by image analysis (ImageJ), and the ratio of the lesion area to the total area was calculated. For the cross-sectional analysis of the aorta, the OCT-embedded aortas were sectioned using a cryostat, and 6- μm sections were obtained sequentially beginning at the aortic valve. Eight sections obtained every 24 μm from the aortic sinus were stained with oil red O and used for the quantification of lesion areas. The lesion areas of each aorta were measured using ImageJ. The average of the 8 sections from 1 mouse was taken as a value that represented the mouse.

Immunohistochemistry

Eight sections of aortic root per mouse were stained with an anti-CD68 antibody (1:200), anti-CD3 antibody (1:50), anti- α smooth muscle actin (SMA) antibody (1:50), anti-ssDNA antibody (1:600), anti-iNOS antibody (1:200), anti-VCAM-1 antibody (1:50), anti-ICAM-1 antibody (1:50), anti-IL-6 antibody (1:400), and anti-IL-10 antibody (1:50). The lesion and positively stained areas of each aorta were measured using ImageJ. The average of the 8 sections from 1 mouse was taken as a value that represented the mouse.

Apoptosis Assay

After being washed 3 times in PBS, peritoneal macrophages were loaded with free cholesterol (FC) by incubation with RPMI1640 containing 10% FBS supplemented with or without 300 $\mu\text{g}/\text{mL}$ of acLDL plus 10 $\mu\text{g}/\text{mL}$ of ACAT inhibitor (58035). The next day, cells were assayed for early- to midstage

apoptosis by staining with Alexa Fluor 488–conjugated annexin V (green), as described previously^{27,33,34}, using a Vybrant Apoptosis Assay Kit (Molecular Probes). Representative fields (4 to 6 fields containing ≈ 1000 cells) were photographed. The number of annexin V–positive cells was counted and expressed as a percentage of the total number of cells in at least 4 separate fields. For Western blotting of cleaved caspase-3, the samples were collected 48 hours after stimulation.

Measurement of Serum ApoA-I Levels

We quantified serum apoA-I levels in mice using an ELISA assay kit for mouse apoA-I in accordance with the manufacturer's instructions (USCN Life Science Inc, Wuhan, China).

Measurement of Total Cholesterol, Free Cholesterol, Cholesterol Ester, and Triglyceride in the Liver

Lipids in the liver were extracted by the Folch procedure³⁵ and quantified using standard enzymatic colorimetric methods.

Statistics

Data are presented as mean \pm SE. Statistical comparisons were performed using nonparametric analysis when the group numbers were <10 (Mann–Whitney *U* test). Otherwise, unpaired 2-tailed Student *t* tests were conducted. Statistical significance was tested by a 1-way analysis of variance with the Bonferroni post hoc test when experiments included >2 groups. The level of significance was set at a probability value of <0.05 .

Results

MiR-33 Deficiency Reduced Atherosclerosis

To clarify the role of miR-33 in the progression of atherosclerosis, miR-33^{-/-} mice²² were mated with *ApoE*^{-/-} mice.^{20,21} Because both lines have a BL/6 background, miR-33^{-/-}*ApoE*^{-/-} double-knockout mice also had a BL/6 background. The miR-33^{-/-}*ApoE*^{-/-} mice were born at the expected Mendelian ratio, and miR-33^{+/+}*ApoE*^{-/-} littermates were used as controls. The miR-33^{+/+}*ApoE*^{-/-} and miR-33^{-/-}*ApoE*^{-/-} mice were fed a WTD containing 0.15% cholesterol

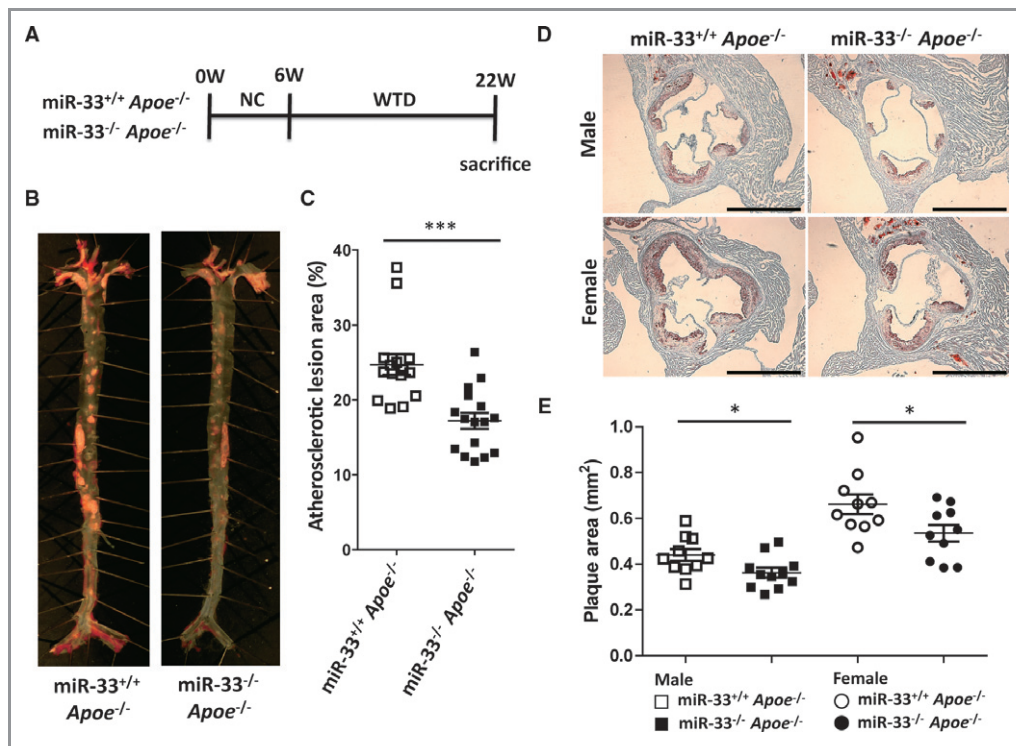


Figure 1. miR-33 deficiency reduced atherosclerosis. A, Experimental protocol for the analysis of atherosclerosis in miR-33^{+/+}*ApoE*^{-/-} and miR-33^{-/-}*ApoE*^{-/-} mice. B, Representative images of the en face analysis of the total aorta in miR-33^{+/+}*ApoE*^{-/-} and miR-33^{-/-}*ApoE*^{-/-} male mice. C, Quantification of the atherosclerotic lesion area in en face analysis of the total aorta in male mice. Values are mean \pm SE (n=15 to 16 each); ****P* <0.001 . D, Representative microscopic images of cross-sections of proximal aorta in miR-33^{+/+}*ApoE*^{-/-} and miR-33^{-/-}*ApoE*^{-/-} male and female mice. Scale bar: 1 mm. E, Quantification of the atherosclerotic plaque area in cross-sections of proximal aorta in male and female mice. Values are mean \pm SE (n=10 to 11 each); **P* <0.05 .

beginning at age 6 weeks, and atherosclerotic lesions were analyzed at age 22 weeks (Figure 1A). The atherosclerotic lesion area was examined by an en face analysis of the total aorta and cross-sections of the proximal aorta. The en face analysis of the total aorta showed that atherosclerotic lesions throughout the aorta were significantly reduced in miR-33^{-/-} *Apoe*^{-/-} mice compared with miR-33^{+/+} *Apoe*^{-/-} mice (male: $P < 0.001$, $24.7 \pm 1.4\%$ versus $17.2 \pm 1.1\%$, Figure 1B and 1C). The plaque area in the proximal aorta was extensively examined in males and females. Atherosclerotic lesions were significantly reduced in miR-33^{-/-} *Apoe*^{-/-} mice of both sexes (male: $P = 0.0314$, 0.44 ± 0.025 versus 0.36 ± 0.021 mm²; female: $P = 0.0372$, 0.66 ± 0.042 versus 0.54 ± 0.036 mm²; Figure 1D and 1E). The plaque area in females was greater than that in males. Moreover, the quantification of lipid accumulation by oil red O staining showed a significant decrease in miR-33^{-/-} *Apoe*^{-/-} compared with miR-33^{+/+} *Apoe*^{-/-} mice ($P = 0.034$, $9.8 \pm 1.1\%$ versus $7.1 \pm 0.5\%$;

Figure 2A and 2B). To further analyze lesion macrophages in these mice, we stained aortic plaque using an anti-CD68 antibody. The CD68-positive area was also significantly decreased in the proximal aortas of miR-33^{-/-} *Apoe*^{-/-} mice compared with miR-33^{+/+} *Apoe*^{-/-} mice ($P = 0.0022$, $24.9 \pm 1.0\%$ versus $20.5 \pm 0.7\%$; Figure 2C and 2D). We also analyzed CD3-positive cells, α SMA-positive area, and picrosirius red staining for collagens (Figure 3A through 3F). CD3-positive cells were significantly reduced in miR-33^{-/-} *Apoe*^{-/-}

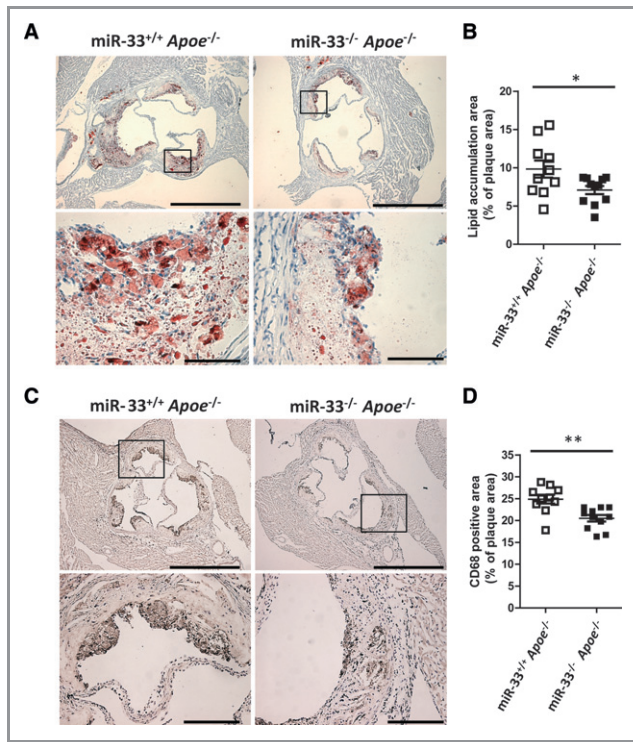


Figure 2. miR-33 deficiency reduced lipid accumulation and macrophage content in atherosclerotic plaque. A, Representative microscopic images of the lipid accumulation area in cross-sections of proximal aorta in miR-33^{+/+} *Apoe*^{-/-} and miR-33^{-/-} *Apoe*^{-/-} male mice. Scale bars: 1 mm (upper), 100 μ m (lower). B, Quantification of lipid accumulation area in cross-sections of proximal aorta in male mice. Values are mean \pm SE (n=10 to 11 each); * $P < 0.05$. C, Representative microscopic images of immunohistochemical staining for the macrophage marker CD68 in male mice. Scale bars: 1 mm (upper), 200 μ m (lower). D, Quantification of the CD68-positive area in cross-sections of proximal aorta in male mice. Values are mean \pm SE (n=10 to 11 each); ** $P < 0.01$.

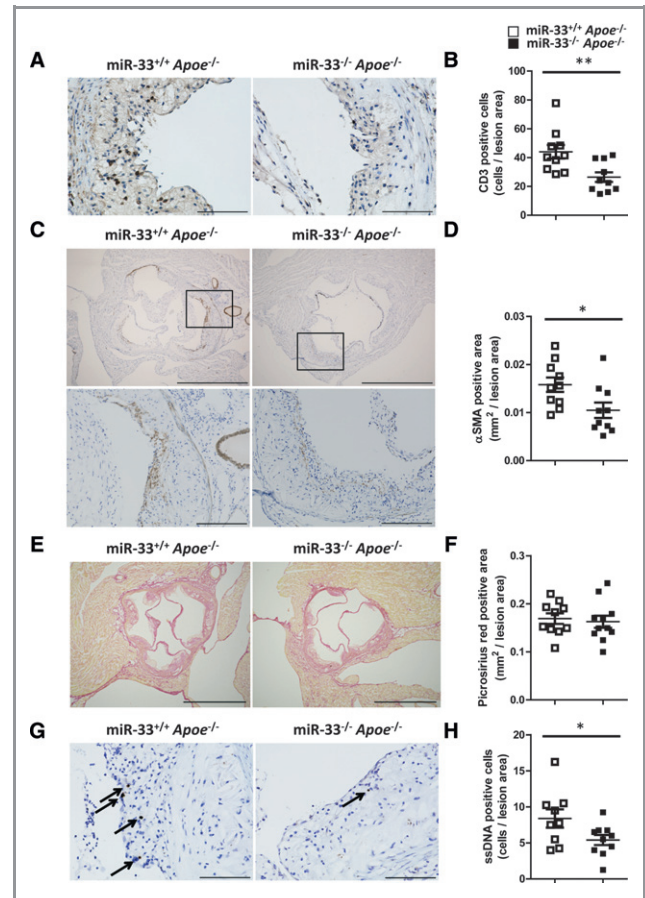


Figure 3. miR-33 deficiency reduced CD3-positive cell accumulation and apoptosis in atherosclerotic plaque. A, Representative microscopic images of immunohistochemical staining for the T-cell marker CD3 in male mice. Scale bar: 100 μ m. B, Quantification of CD3-positive cells in cross-sections of proximal aorta in male mice. Values are mean \pm SE (n=10 each); ** $P < 0.01$. C, Representative microscopic images of immunohistochemical staining for α SMA in male mice. Scale bars: 1 mm (upper), 200 μ m (lower). D, Quantification of the α SMA-positive area in cross-sections of proximal aorta in male mice. Values are mean \pm SE (n=10 each); * $P < 0.05$. E, Representative microscopic images of picrosirius red staining for the collagen in male mice. Scale bar: 1 mm. F, Quantification of the picrosirius red-positive area in cross-sections of proximal aorta in male mice. Values are mean \pm SE (n=10 to 11 each). G, Representative microscopic images of immunohistochemical staining for ssDNA in male mice. Scale bar: 100 μ m. H, Quantification of ssDNA-positive cells in cross-sections of proximal aorta in male mice. Values are mean \pm SE (n=9 to 10 each); * $P < 0.05$.

compared with miR-33^{+/+}*ApoE*^{-/-} mice ($P=0.0066$; Figure 3A and 3B). The α SMA-positive area was also significantly reduced in miR-33^{-/-}*ApoE*^{-/-} mice ($P=0.025$ Figure 3C and 3D). However, no difference was noted in the collagen area (Figure 3E and 3F). There was a significant reduction in lesional apoptosis, as measured by anti-ssDNA staining ($P=0.0493$; Figure 3G and 3H). These results indicated that a deficiency of miR-33 decreased atherosclerotic plaque size and lipid content and reduced the accumulation of macrophages and T cells in atherosclerotic plaques.

MiR-33 Deficiency Increased HDL-C

We previously reported that miR-33^{-/-} mice showed 22% to 39% higher serum HDL-C levels than wild-type mice.²² We measured HDL-C levels in the serum of miR-33^{+/+}*ApoE*^{-/-} and miR-33^{-/-}*ApoE*^{-/-} mice at the time of euthanization by the standard method. HDL-C was significantly elevated in miR-33^{-/-}*ApoE*^{-/-} mice compared with miR-33^{+/+}*ApoE*^{-/-} mice of both sexes (Figure 4A). We further classified and quantified serum lipoproteins by high-performance liquid chromatography (HPLC). Representative results of the HPLC elution profile of serum of both sexes are shown in Figure 4B and 4C, and lipid profiles are summarized in Table 1. These results show

that only the HDL-C level differed between the serum of miR-33^{+/+}*ApoE*^{-/-} and miR-33^{-/-}*ApoE*^{-/-} mice. Serum apoA-I levels are shown in Figure 4D. To assess the cholesterol efflux capacity of the serum, cholesterol efflux via apolipoprotein B (apoB)-depleted serum was measured using ³H-cholesterol-labeled J774 mouse macrophages. The mean values of serum HDL-C used in this experiment were 17.8±1.4 versus 19.5±1.8 mg/dL in males and 10.2±0.5 versus 17.3±1.7 mg/dL in females (miR-33^{+/+}*ApoE*^{-/-} versus miR-33^{-/-}*ApoE*^{-/-} mice, $n=6$ for each group). ApoB-depleted serum from miR-33^{-/-}*ApoE*^{-/-} mice significantly promoted cholesterol efflux in J774 macrophages (Figure 4E). These results indicated that deficiency of miR-33 elevated serum cholesterol efflux capacity, possibly through the elevation of HDL-C levels.

Peritoneal Macrophages From MiR-33^{-/-}*ApoE*^{-/-} Mice Showed Improved Cholesterol Efflux

To characterize the function of macrophages in cholesterol efflux, thioglycollate-elicited peritoneal macrophages (PEMs) were isolated from mice. Previously, we and others have shown that miR-33 targeted the 3' untranslated region (UTR) of *Abca1* and *Abcg1*.^{16–18,22} mRNA expression of ABCA1 and protein expression of ABCA1 and ABCG1 were significantly increased in

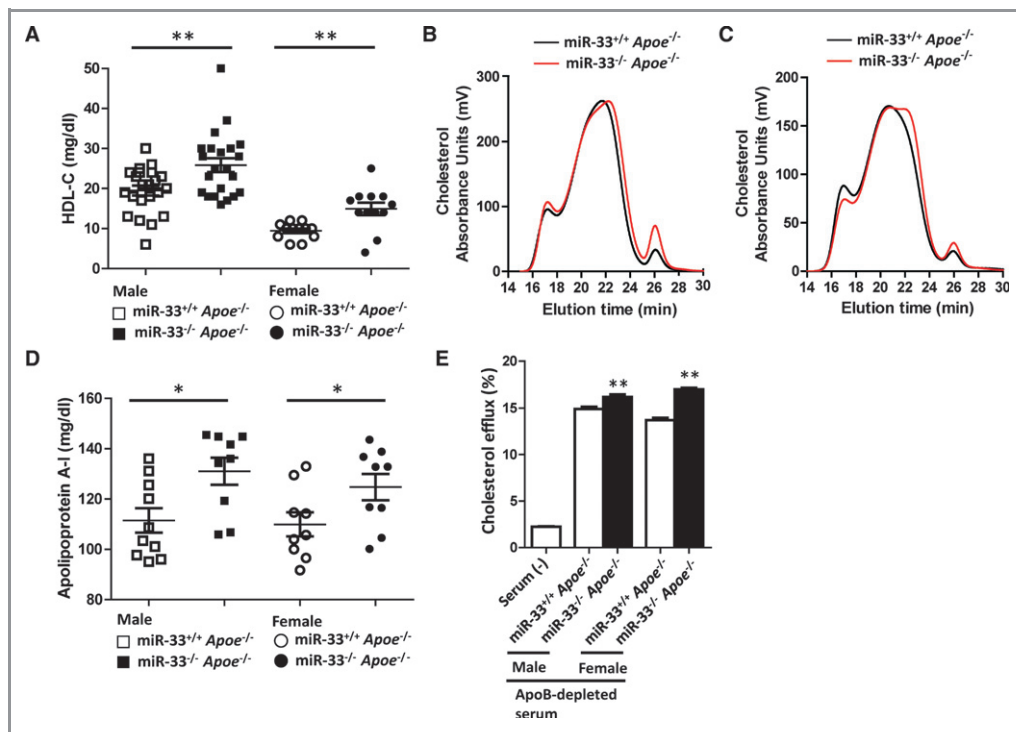


Figure 4. miR-33 deficiency increased HDL-C. A, Serum HDL-C levels determined by standard methods in miR-33^{+/+}*ApoE*^{-/-} and miR-33^{-/-}*ApoE*^{-/-} male and female mice. Values are mean±SE (male, $n=22$; female, $n=11$ each); ** $P<0.01$. B, Representative HPLC analysis of serum cholesterol from male miR-33^{+/+}*ApoE*^{-/-} and miR-33^{-/-}*ApoE*^{-/-} mice. C, Representative HPLC analysis of serum cholesterol from female miR-33^{+/+}*ApoE*^{-/-} and miR-33^{-/-}*ApoE*^{-/-} mice. D, Serum apoA-I levels in miR-33^{+/+}*ApoE*^{-/-} and miR-33^{-/-}*ApoE*^{-/-} mice; * $P<0.05$. E, Cholesterol efflux via apoB-depleted serum from miR-33^{+/+}*ApoE*^{-/-} and miR-33^{-/-}*ApoE*^{-/-} mice using ³H-cholesterol-labeled J774 mouse macrophages. Values are mean±SE ($n=6$ each); ** $P<0.01$. HDL-C indicates high-density lipoprotein cholesterol; HPLC, high-performance liquid chromatography.

Table 1. Serum Lipid Profiling of miR-33^{+/+}Apoe^{-/-} and miR-33^{-/-}Apoe^{-/-} Mice by HPLC

	Lipoprotein		Male		Female	
	Major (Fraction No.) Diameter	Subclass (Fraction No.)	miR-33 ^{+/+} Apoe ^{-/-}	miR-33 ^{-/-} Apoe ^{-/-}	miR-33 ^{+/+} Apoe ^{-/-}	miR-33 ^{-/-} Apoe ^{-/-}
TC, mg/dL			705.3±72.1	768.4±45.2	598.9±88.8	574.2±70.0
	CM (1 to 2), >80 nm		129.2±21.6	157.9±19.8	124.6±20.9	138.6±28.11
	VLDL (3 to 7), 30 to 80 nm		419.5±44.1	450.9±30.0	353.6±51.7	322.1±36.4
		Large VLDL (3 to 5)	279.3±32.2	316.4±24.9	245.1±35.1	230.2±29.5
		Medium VLDL (6)	100.5±9.8	96.77±5.67	79.04±12.17	66.37±6.15
		Small VLDL (7)	39.74±3.31	37.75±1.47	29.47±4.87	25.6±2.12
	LDL (8 to 13), 16 to 30 nm		133.8±14.9	126.4±5.23	103.0±16.2	90.81±6.72
		Large LDL (8)	47.47±4.40	44.05±1.53	36.58±6.03	31.60±2.61
		Medium LDL (9)	39.93±4.56	36.35±1.71	31.99±5.26	27.53±2.11
		Small LDL (10)	25.63±3.42	24.72±1.49	19.78±3.05	17.36±1.23
		Very small LDL (11 to 13)	20.75±2.75	21.25±1.19	14.65±1.89	14.33±1.27
	HDL (14 to 20), 8 to 16 nm		22.79±1.28	33.21±2.51**	17.62±0.73	22.71±2.52*
		Very large HDL (14 to 15)	3.04±0.39	3.66±0.17	3.57±0.42	3.89±0.56
		Large HDL (16)	5.88±0.63	9.39±0.87**	4.00±0.28	5.29±0.47*
		Medium HDL (17)	8.04±0.71	11.88±1.21*	4.49±0.36	6.79±0.26**
		Small HDL (18)	2.61±0.12	3.73±0.30**	2.16±0.13	2.87±0.36
		Very small HDL (19 to 20)	3.23±0.25	4.55±0.27**	3.40±0.45	3.87±0.61
TG, mg/dL			39.94±8.29	48.32±10.14	17.60±1.44	24.75±5.19

Values are mean±SEM. After a 4-hour fast, blood was obtained from mice fed a WTD for 16 weeks (male, n=6 each; female, n=5 each). The serum was analyzed by HPLC, as described in Methods. TC indicates total cholesterol; TG, triglyceride; CM, chylomicrons; VLDL, very low-density lipoprotein; LDL, low-density lipoprotein; HDL, high-density lipoprotein.

*P<0.05, **P<0.01 compared with miR-33^{+/+}Apoe^{-/-} mice.

PEMs from miR-33^{-/-}Apoe^{-/-} mice compared with PEMs from miR-33^{+/+}Apoe^{-/-} mice (Figure 5A and 5B). To test the hypothesis that enhanced cholesterol efflux in macrophages contributed to the reduction in the development of atherosclerosis in miR-33^{-/-}Apoe^{-/-} mice, cholesterol efflux to apoA-I and HDL-C was measured using ³H-cholesterol-labeled acetylated low-density lipoprotein (acLDL). Both apoA-I- and HDL-C-mediated cholesterol efflux were significantly elevated in macrophages from miR-33^{-/-}Apoe^{-/-} compared with macrophages from miR-33^{+/+}Apoe^{-/-} mice in a dose-dependent manner (Figure 5C and 5D). These results indicate that miR-33 deficiency improved macrophage cholesterol efflux by increasing the expressions of macrophage ABCA1 and ABCG1.

miR-33 Deficiency Affected Circulating Monocytes and Lesional Macrophages

Our findings thus far indicate that miR-33 deficiency reduced the accumulation of inflammatory cells in atherosclerotic plaque. We then examined whether miR-33 deficiency influenced the monocyte count or subset frequency in peripheral blood. The total leukocyte count in miR-33^{-/-}Apoe^{-/-} mice was significantly less than that in miR-33^{+/+}Apoe^{-/-} mice

(Figure 6A). Blood monocyte subsets were discriminated by flow cytometry on the basis of their expression of CD115 and Ly6C.³⁶ The frequency of proinflammatory Ly6C^{high} monocytes in miR-33^{-/-}Apoe^{-/-} mice was significantly higher than that in miR-33^{+/+}Apoe^{-/-} mice (Figure 6B through 6E). We further measured iNOS, interleukin (IL)-6, and IL-10 expression in atherosclerotic plaque by immunohistochemistry. As shown in Figure 7A and 7B, the iNOS-positive area in atherosclerotic plaque in miR-33^{-/-}Apoe^{-/-} mice was significantly less than that in miR-33^{+/+}Apoe^{-/-} mice (P=0.0057). On the other hand, no differences were observed in IL-6 and IL-10 immunostaining (Figure 7C through 7F). We also characterized miR-33^{-/-}Apoe^{-/-} macrophages by analyzing the expression of classically activated or proinflammatory (M1) and alternatively activated or anti-inflammatory (M2) macrophage markers using mouse PEMs. A previous article indicated that the inhibition of miR-33 by antisense oligonucleotide enhanced M2 marker expression in macrophages.¹⁹ However, our experiments indicated that the mRNA levels of both M2 markers such as *IL-10* and *Chi3l3* mRNA and an M1 marker such as *IL-6* in PEMs from miR-33^{-/-}Apoe^{-/-} mice were significantly elevated compared with those from miR-33^{+/+}Apoe^{-/-} mice (Figure 7G). Overall, these results

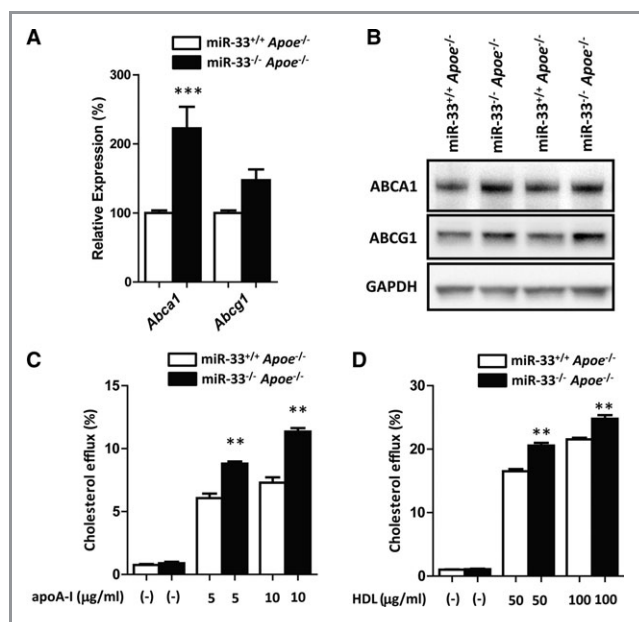


Figure 5. miR-33 deficiency improved cholesterol efflux in macrophages. A, Quantitative real-time PCR analysis of *Abca1* and *Abcg1* in macrophages from miR-33^{+/+}*Apoe*^{-/-} and miR-33^{-/-}*Apoe*^{-/-} mice. Values from miR-33^{+/+}*Apoe*^{-/-} were set at 100%. Values are mean±SE (n=7 each); ****P*<0.001. B, Western blotting analysis of ABCA1 and ABCG1 in thioglycollate-elicited peritoneal macrophages from miR-33^{+/+}*Apoe*^{-/-} and miR-33^{-/-}*Apoe*^{-/-} mice. GAPDH was used as a loading control. C, Cholesterol efflux from thioglycollate-elicited peritoneal macrophages in the presence or absence of apoA-I (5 or 10 µg/mL). Values are mean±SE (n=6 each); ***P*<0.01. D, Cholesterol efflux from thioglycollate-elicited peritoneal macrophages in the presence or absence of HDL-C (50 or 100 µg/mL). Values are mean±SE (n=6 each); ***P*<0.01.

demonstrate that a loss of miR-33 may have affected multiple pathways in both pro- and anti-inflammatory processes. Moreover, we analyzed adhesion molecule expression by immunostaining. As shown in Figure 8A and 8B, the VCAM-1-positive area in atherosclerotic plaque in miR-33^{-/-}*Apoe*^{-/-} was significantly less than that in miR-33^{+/+}*Apoe*^{-/-} mice (*P*=0.0008). The ICAM-1-positive area in miR-33^{-/-}*Apoe*^{-/-} mice tended to be less than that in miR-33^{+/+}*Apoe*^{-/-} mice (*P*=0.127), shown in Figure 8C and 8D.

MiR-33 Target Genes Were Altered in the Livers of MiR-33^{-/-} Mice on an *Apoe*^{-/-} Background

It has already been shown that miR-33 targets several genes that affect cholesterol and fatty acid synthesis. We measured the mRNA and protein levels of ABCA1, CROT, and CPT1a in the livers of these mice. As shown in Figure 9A through 9C, mRNA of CROT and protein levels of ABCA1 and CROT in miR-33^{-/-}*Apoe*^{-/-} mice were significantly elevated compared with those in miR-33^{+/+}*Apoe*^{-/-} mice. No differences were observed in CPT1a and AMPK α expressions. Next, we measured the lipid

content in the liver. However, there was no difference in total cholesterol, free cholesterol, cholesterol ester, or triglyceride levels in the livers of miR-33^{+/+}*Apoe*^{-/-} mice and miR-33^{-/-}*Apoe*^{-/-} mice (Figure 9D). No apparent changes in histology were observed in the livers of these mice, as shown by HE staining (Figure 9E). Moreover, we measured the level of RIP140 (NRIP1), which has been shown to be one of the targets of miR-33 in macrophages of these mice.³⁷ Protein level of RIP140 in miR-33^{-/-}*Apoe*^{-/-} macrophages was significantly increased compared with that in miR-33^{+/+}*Apoe*^{-/-} macrophages (Figure 9F through 9H), which may be one of the reasons why the expression of inflammatory cytokine such as IL-6 in PEMs of miR-33^{-/-}*Apoe*^{-/-} mice was increased compared with that in miR-33^{+/+}*Apoe*^{-/-} mice.³⁸

Loss of MiR-33 in Blood Cells Did Not Alter Serum HDL-C Levels

The results of these experiments show that both the rise in HDL-C level and the improvement in macrophage cholesterol efflux may have contributed to the reduction in atherosclerotic plaques. To elucidate the contribution of miR-33 in macrophages to the development of atherosclerosis in vivo, we used bone marrow transplantation (BMT) to generate *Apoe*^{-/-} mice selectively deficient in leukocyte miR-33. Male mice with miR-33^{+/+}*Apoe*^{-/-} or miR-33^{-/-}*Apoe*^{-/-} genotypes (8 weeks old) were used as bone marrow (BM) donors. BM recipients were female miR-33^{+/+}*Apoe*^{-/-} mice (8 weeks old). Thus, all the mice used for BMT had an *Apoe*^{-/-} background. After BMT, mice were fed NC for 4 weeks and then switched to a WTD for 12 weeks. At age 24 weeks, mice were euthanized and analyzed (Figure 10A). Successful hematopoietic reconstitution after BMT was confirmed by PCR amplification of the whole-blood genome 4 weeks after BMT and by PCR amplification of the BM and tail genomes at the time of euthanization. MiR-33 was barely detectable in BM cells from miR-33^{-/-}*Apoe*^{-/-} BM recipients by quantitative PCR analysis for miR-33 (data not shown). The serum lipid profile of recipient mice is shown in Table 2. Serum HDL-C levels of miR-33^{+/+}*Apoe*^{-/-} BM recipients were the same as those in miR-33^{-/-}*Apoe*^{-/-} BM recipients, which were similar to the levels in miR-33^{+/+}*Apoe*^{-/-} mice in Figure 4A. These results indicated that miR-33 expression in macrophages did not contribute to serum HDL-C levels, which is consistent with the results that the liver and intestine are the major sources of HDL-C.^{39,40}

MiR-33^{+/+}*Apoe*^{-/-} Mice Transplanted With MiR-33^{-/-}*Apoe*^{-/-} BM Had Reduced Lipid Accumulation in Atherosclerotic Plaque

After mice were fed a WTD for 12 weeks, atherosclerotic lesions in the proximal aortas were measured. Atherosclerotic

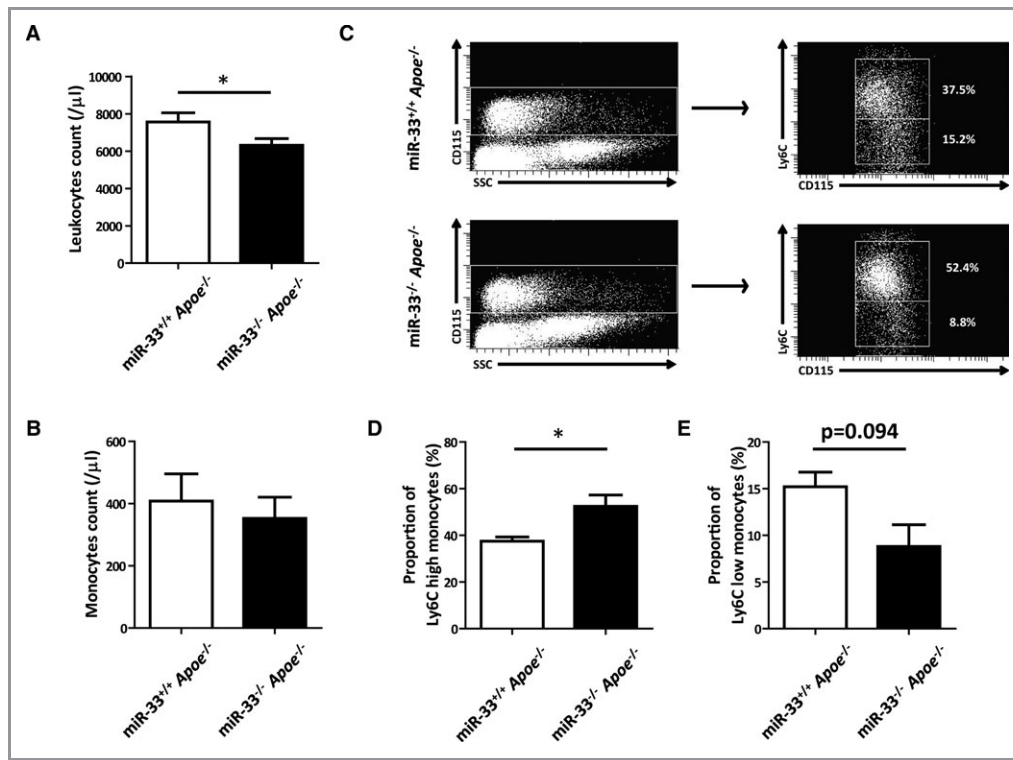


Figure 6. miR-33^{-/-}ApoE^{-/-} mice had reduced leukocyte numbers in peripheral blood and a greater Ly-6C^{high} monocyte subset compared with miR-33^{+/+}ApoE^{-/-} mice. A, Leukocyte count in peripheral blood in miR-33^{+/+}ApoE^{-/-} and miR-33^{-/-}ApoE^{-/-} mice. Values are mean±SE (n=15 to 16 each); *P<0.05. B, Numbers of monocyte in peripheral blood in miR-33^{+/+}ApoE^{-/-} and miR-33^{-/-}ApoE^{-/-} mice. Values are mean±SE (n=9 each). C, Scheme for gating of monocytes using an anti-CD115 antibody, and representative dot plots showing the quantification of Ly-6C^{high} and Ly-6C^{low} monocyte subsets in miR-33^{+/+}ApoE^{-/-} and miR-33^{-/-}ApoE^{-/-} mice. D, Proportion of the Ly-6C^{high} monocyte subset to total monocytes in miR-33^{+/+}ApoE^{-/-} and miR-33^{-/-}ApoE^{-/-} mice. Values are mean±SE (n=9 each.); *P<0.05. E, Proportion of the Ly-6C^{low} monocyte subset to total monocytes in miR-33^{+/+}ApoE^{-/-} and miR-33^{-/-}ApoE^{-/-} mice. Values are mean±SE (n=9 each).

plaque formation in mice transplanted with miR-33^{-/-}ApoE^{-/-} BM tended to be reduced compared with that in mice transplanted with miR-33^{+/+}ApoE^{-/-} BM, but this difference was not statistically significant ($P=0.12$, 0.53 ± 0.028 versus 0.46 ± 0.033 mm²; Figure 10B and 10C). On the other hand, the quantification of lipid accumulation by oil red O staining showed a significant decrease in mice transplanted with miR-33^{-/-}ApoE^{-/-} BM compared with mice with miR-33^{+/+}ApoE^{-/-} BM ($P=0.020$, $3.0\pm 0.4\%$ versus $1.9\pm 0.2\%$; Figure 10D and 10E). The CD68-positive area is shown in Figure 10F and 10G ($P=0.09$, $19.5\pm 2.6\%$ versus $26.6\pm 2.6\%$). These results showed that loss of miR-33 in blood cells reduced the lipid content of atherosclerotic plaque.

Free Cholesterol–Induced Apoptosis Was Reduced in PEMs From MiR-33^{-/-}ApoE^{-/-} Mice Compared With MiR-33^{+/+}ApoE^{-/-} Mice

Because mice transplanted with miR-33^{-/-}ApoE^{-/-} BM showed reduced lipid accumulation in atherosclerotic plaque compared with mice transplanted with miR-33^{+/+}ApoE^{-/-}

BM, we analyzed free cholesterol (FC)–induced apoptosis in PEMs by treating macrophages with acLDL and acyl-CoA: cholesterol acyl-transferase (ACAT) inhibitor. Figure 11A shows the results of annexin V staining of PEMs with and without acLDL plus ACAT inhibitor treatment. Annexin V–positive cells were significantly increased in PEMs from miR-33^{+/+}ApoE^{-/-} mice compared with those from miR-33^{-/-}ApoE^{-/-} mice after FC loading (Figure 11B). Cleaved caspase-3 was also increased in PEMs from miR-33^{+/+}ApoE^{-/-} mice compared with those from miR-33^{-/-}ApoE^{-/-} mice after FC loading (Figure 11C).

MiR-33^{-/-}ApoE^{-/-} Mice Transplanted With BM of MiR-33^{+/+}ApoE^{-/-} or MiR-33^{-/-}ApoE^{-/-} Showed Only a Slight Increase in HDL-C Levels Compared With MiR-33^{+/+}ApoE^{-/-} Mice Transplanted With BM of MiR-33^{+/+}ApoE^{-/-} or MiR-33^{-/-}ApoE^{-/-}

Previous experiments indicated that loss of miR-33 in blood cells reduced lipid accumulation in atherosclerotic plaque.

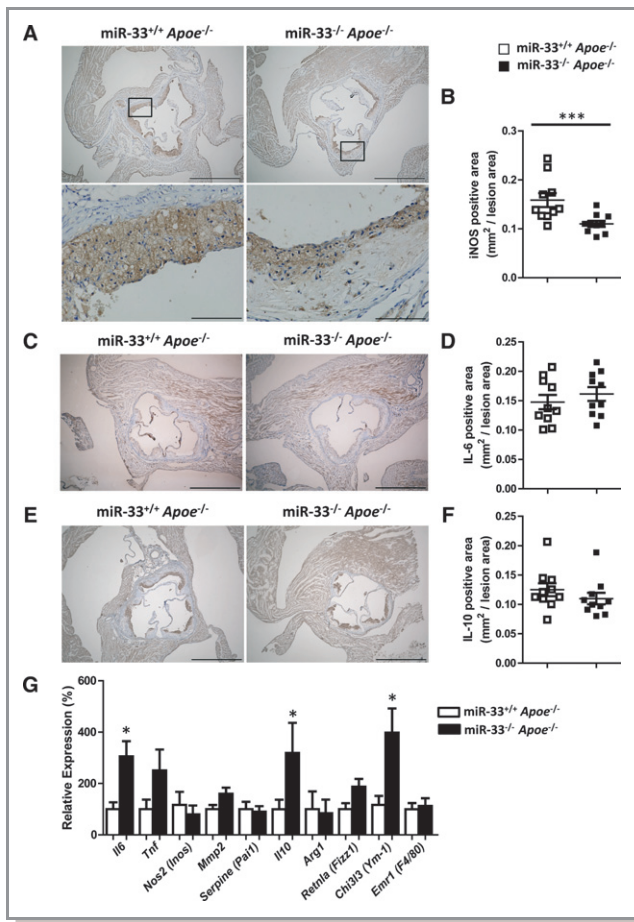


Figure 7. miR-33 deficiency reduced the iNOS-positive areas in atherosclerotic plaque and induced coordinated M1 and M2 marker expression in PEMs. A, Representative microscopic images of immunohistochemical staining for iNOS in male mice. Scale bars: 1 mm (upper), 100 μ m (lower). B, Quantification of the iNOS-positive area in cross-sections of proximal aorta in male mice. Values are mean \pm SE (n=10 each); *** P <0.001. C, Representative microscopic images of immunohistochemical staining for IL-6 in male mice. Scale bar: 1 mm. D, Quantification of the IL-6-positive area in cross-sections of proximal aorta in male mice. Values are mean \pm SE (n=10 each). E, Representative microscopic images of immunohistochemical staining for IL-10 in male mice. Scale bar: 1 mm. F, Quantification of the IL-10-positive area in cross-sections of proximal aorta in male mice. Values are mean \pm SE (n=10 each). G, Quantitative real-time PCR analysis of proinflammatory (M1) and anti-inflammatory (M2) markers in residual PEMs from miR-33^{+/+}Apoe^{-/-} and miR-33^{-/-}Apoe^{-/-} mice. Values from miR-33^{+/+}Apoe^{-/-} mice were set at 100%. Values are mean \pm SE (n=7 each); * P <0.05.

Next, to determine the contribution of miR-33 deficiency to atherosclerosis in BM recipients, we transferred BM of miR-33^{+/+}Apoe^{-/-} or miR-33^{-/-}Apoe^{-/-} mice to miR-33^{-/-}Apoe^{-/-} mice in the same way as in the previous BMT experiments (Figure 12A). However, the HDL-C levels in miR-33^{-/-}Apoe^{-/-} mice transplanted with BM of miR-33^{+/+}Apoe^{-/-} or miR-33^{-/-}Apoe^{-/-} (Table 3) showed only a

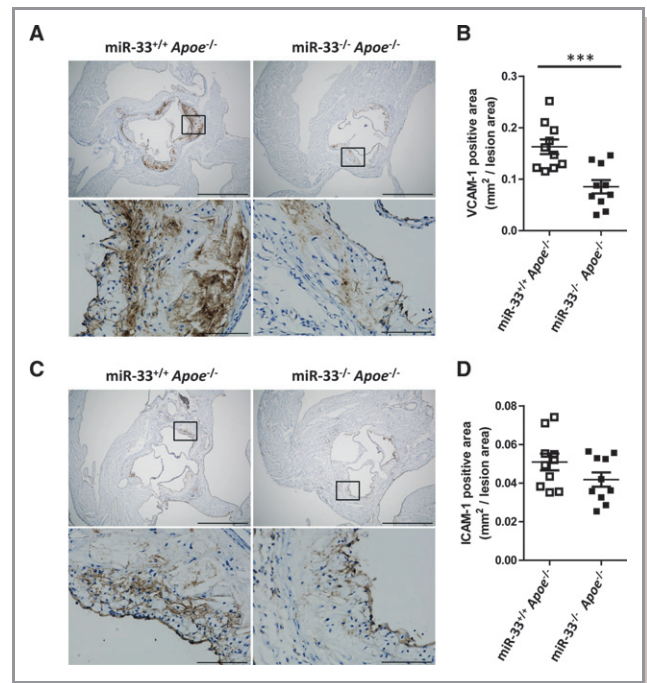


Figure 8. miR-33 deficiency reduced the VCAM-1-positive area in atherosclerotic plaque. A, Representative microscopic images of immunohistochemical staining for VCAM-1 in male mice. Scale bars: 1 mm (upper), 100 μ m (lower). B, Quantification of the VCAM-1-positive area in cross-sections of proximal aorta in male mice. Values are mean \pm SE (n=10 each); *** P <0.001. C, Representative microscopic images of immunohistochemical staining for ICAM-1 in male mice. Scale bars: 1 mm (upper), 100 μ m (lower). D, Quantification of the ICAM-1-positive area in cross-sections of proximal aorta in male mice. Values are mean \pm SE (n=10); P =0.127.

slight increase compared with miR-33^{+/+}Apoe^{-/-} mice transplanted with BM of miR-33^{+/+}Apoe^{-/-} or miR-33^{-/-}Apoe^{-/-} (Table 2). Therefore, it was impossible to observe an effect of HDL-C elevation caused by the loss of miR-33 on atherosclerosis in recipients that had the same type of blood cells (Figures 10 and 12).

MiR-33^{-/-}Apoe^{-/-} Mice Transplanted With MiR-33^{-/-}Apoe^{-/-} BM Had Reduced Lipid Accumulation in Atherosclerotic Plaque

We also observed the effect of loss of miR-33 in BMT experiments in miR-33^{-/-}Apoe^{-/-} recipients. Atherosclerotic plaque formation in miR-33^{-/-}Apoe^{-/-} mice transplanted with miR-33^{-/-}Apoe^{-/-} BM was comparable with that in miR-33^{-/-}Apoe^{-/-} mice transplanted with miR-33^{+/+}Apoe^{-/-} BM (0.46 \pm 0.023 versus 0.42 \pm 0.020 mm²; Figure 12B and 12C). Although the area of lipid accumulation in miR-33^{-/-}Apoe^{-/-} mice transplanted with miR-33^{-/-}Apoe^{-/-} BM was significantly reduced compared with that in miR-33^{-/-}Apoe^{-/-} mice transplanted with miR-33^{+/+}

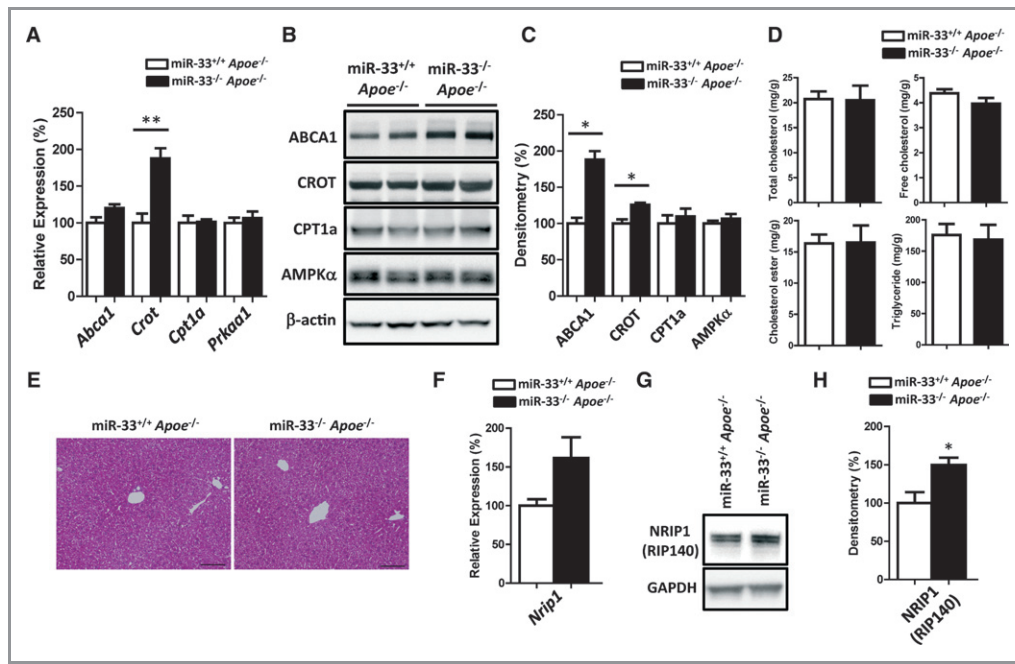


Figure 9. Expression of ABCA1 and CROT in livers and RIP140 in macrophages is elevated in miR-33^{-/-} ApoE^{-/-} mice compared with miR-33^{+/+} ApoE^{-/-} mice. A, Quantitative real-time PCR analysis of *Abca1*, *Crot*, *Cpt1a*, and *Prkaa1* in livers from miR-33^{+/+} ApoE^{-/-} and miR-33^{-/-} ApoE^{-/-} mice. Values from miR-33^{+/+} ApoE^{-/-} mice were set at 100%. Values are mean±SE (n=9 to 11 each); **P<0.01. B, Western analysis of ABCA1, CROT, CPT1a, and AMPKα in livers from miR-33^{+/+} ApoE^{-/-} and miR-33^{-/-} ApoE^{-/-} mice. β-actin was used as a loading control. C, Densitometry of ABCA1, CROT, CPT1a, and AMPKα in livers from miR-33^{+/+} ApoE^{-/-} and miR-33^{-/-} ApoE^{-/-} mice. Values from miR-33^{+/+} ApoE^{-/-} mice were set at 100%. Values are mean±SE (n=4 each); *P<0.05. D, Total cholesterol, free cholesterol, cholesterol ester, and triglyceride levels in livers of miR-33^{+/+} ApoE^{-/-} and miR-33^{-/-} ApoE^{-/-} mice. Values are mean±SE (n=9 to 11 each). E, HE staining of livers of miR-33^{+/+} ApoE^{-/-} and miR-33^{-/-} ApoE^{-/-} mice at age 20 weeks fed NC. Scale bar: 100 μm. F, Quantitative real-time PCR analysis of *Nrip1* (RIP140) in peritoneal macrophages from miR-33^{+/+} ApoE^{-/-} and miR-33^{-/-} ApoE^{-/-} mice. Values from miR-33^{+/+} ApoE^{-/-} mice were set at 100%. Values are mean±SE (n=7 each). G, Western analysis of NRIP1 (RIP140) in peritoneal macrophages from miR-33^{+/+} ApoE^{-/-} and miR-33^{-/-} ApoE^{-/-} mice. GAPDH was used as a loading control. H, Densitometry of NRIP1 (RIP140) in peritoneal macrophages from miR-33^{+/+} ApoE^{-/-} and miR-33^{-/-} ApoE^{-/-} mice. Values from miR-33^{+/+} ApoE^{-/-} mice were set at 100%. Values are mean±SE (n=4 each); *P<0.05.

ApoE^{-/-} BM (P=0.027, 3.4±0.3% versus 2.2±0.3%; Figure 12D and 12E), there was no difference between these mice in the CD68-positive area (P=0.37, 35.3±3.5% versus 41.2±3.3%; Figure 12F and 12G).

Discussion

In the current study, miR-33^{-/-} ApoE^{-/-} mice showed an increase in HDL-C in vivo and a decrease in atherosclerotic plaque size and lipid content compared with miR-33^{+/+} ApoE^{-/-} mice. Although a previous study demonstrated that the short-term administration of anti-miR-33 oligonucleotides raised HDL-C levels and promoted the regression of atherosclerosis, this current study indicates that miR-33 deficiency contributes to the reduction of plaque size in the progression of advanced atherosclerosis. Moreover, we assessed the in vivo function of miR-33 deficiency in leukocytes by BMT from miR-33^{+/+} ApoE^{-/-} or miR-33^{-/-} ApoE^{-/-} mice into miR-33^{+/+} ApoE^{-/-} or miR-33^{-/-} ApoE^{-/-} mice. miR-33^{-/-} ApoE^{-/-} macrophages promoted the

removal of intracellular lipid content compared with miR-33^{+/+} ApoE^{-/-} macrophages. Together, these data demonstrate that miR-33 deficiency serves to raise HDL-C, improve cholesterol efflux in macrophages, and prevent the progression of atherosclerosis and suggest that miR-33 should be considered as a potential target to prevent the progression of atherosclerosis.

We reported previously that miR-33^{-/-} in C57/BL6 mice increases HDL-C by up to 40%. MiR-33^{-/-} ApoE^{-/-} mice also had a higher amount of HDL-C compared with controls. However, the static measurement of HDL-C cholesterol level has inherent limitations as a metric of the functional effects of HDL-C in vivo. Moreover, HDL-C function in ApoE^{-/-} mice may be altered because these mice had no apoE to activate lecithin: cholesterol acyltransferase, which converts free cholesterol to cholesterol ester, thereby creating a gradient for free cholesterol efflux from cells to HDL-C. Thus, we tried to measure the function of HDL-C from miR-33^{-/-} ApoE^{-/-} mice. Recently, the functionality of HDL-C was analyzed by the quantification of efflux capacity from blood samples of humans.²⁵ Therefore, we

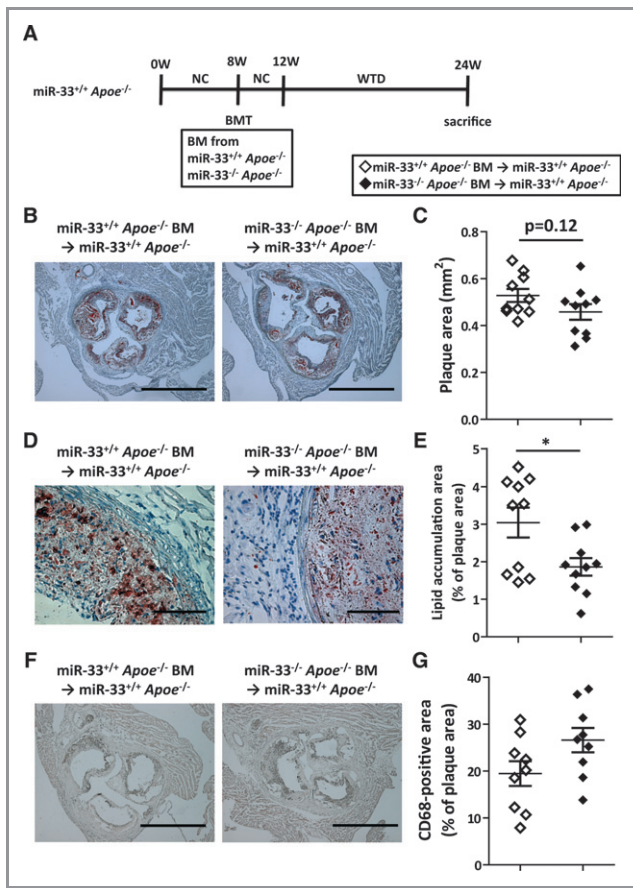


Figure 10. Lipid accumulation area in atherosclerotic lesions was reduced in miR-33^{+/+}Apoe^{-/-} mice transplanted with miR-33^{-/-}Apoe^{-/-} BM. A, Experimental protocol for bone marrow transplantation from miR-33^{+/+}Apoe^{-/-} and miR-33^{-/-}Apoe^{-/-} mice to miR-33^{+/+}Apoe^{-/-} mice. B, Representative microscopic images of cross-sections of proximal aorta in mice transplanted with miR-33^{+/+}Apoe^{-/-} and miR-33^{-/-}Apoe^{-/-} BM. Scale bar: 1 mm. C, Quantification of the atherosclerotic plaque area in cross-sections of proximal aorta. Values are mean±SE (n=10 each). D, Representative microscopic images of the lipid accumulation area in atherosclerotic lesions in mice transplanted with miR-33^{+/+}Apoe^{-/-} and miR-33^{-/-}Apoe^{-/-} BM. Scale bar: 100 μm. E, Quantification of the lipid accumulation area in cross-sections of proximal aorta. Values are mean±SE (n=10 each); *P<0.05. F, Representative microscopic images of immunohistochemical staining for the macrophage marker CD68 in mice transplanted with miR-33^{+/+}Apoe^{-/-} and miR-33^{-/-}Apoe^{-/-} BM. Scale bar: 1 mm. G, Quantification of CD68-positive area in cross-sections of proximal aorta. Values are mean±SE (n=9 each). BM indicates bone marrow.

measured cholesterol efflux capacity in the serum from miR-33^{+/+}Apoe^{-/-} and miR-33^{-/-}Apoe^{-/-} mice. We found that the loss of miR-33 significantly increased the capacity to promote cholesterol efflux, and this may have contributed to the reduction in atherosclerotic plaque volume.

The results of the present BMT experiment revealed that deletion of macrophage miR-33 significantly reduced the lipid

content in atherosclerotic plaque. Macrophages are known to ingest apoB-containing lipoproteins and transport ingested lipoprotein-cholesterol from late endosomes to the endoplasmic reticulum (ER) under normal conditions.⁴¹ In advanced lesional macrophages, the accumulation of massive unesterified, or “free,” cholesterol is observed, which induces ER-stress-mediated macrophage apoptosis.^{42,43} Therefore, we compared atherogenic lipid-induced apoptosis in miR-33^{+/+}Apoe^{-/-} and miR-33^{-/-}Apoe^{-/-} macrophages. Treatment of PEMs in culture with acLDL plus ACAT inhibitor (free cholesterol loading) demonstrated that PEMs from miR-33^{-/-}Apoe^{-/-} mice were significantly resistant to apoptosis compared with those from miR-33^{+/+}Apoe^{-/-} mice. In accordance with this in vitro experiment, apoptotic cells in the lesion area were also reduced in miR-33^{-/-}Apoe^{-/-} mice. It is generally considered that apoptosis of macrophages in advanced plaques may lead to plaque rupture. Thus, the suppression of miR-33 in macrophages may also be beneficial for the prevention of plaque rupture.

To further elucidate the effect of miR-33 deletion on the monocyte/macrophage phenotype, we performed a flow-cytometric analysis of circulating monocytes and a quantitative PCR analysis of RNA from PEMs of miR-33^{+/+}Apoe^{-/-} and miR-33^{-/-}Apoe^{-/-} mice. We first determined that the total leukocyte count in miR-33^{-/-}Apoe^{-/-} mice was less than that in miR-33^{+/+}Apoe^{-/-} mice. This was consistent with a previous report that ABCA1, ABCG1, and HDL inhibit the proliferation of hematopoietic stem cells.⁴⁴ Because leukocytosis enhances the progression of atherosclerosis, the reduction in leukocytes observed in miR-33^{-/-}Apoe^{-/-} mice may have had a beneficial effects on atherosclerosis.⁴⁵ However, we also detected a higher frequency of Ly6C^{high} monocytes in miR-33^{-/-}Apoe^{-/-} mice than in miR-33^{+/+}Apoe^{-/-} mice, and this could enhance inflammation in atherosclerotic plaque. Tissue macrophages are phenotypically heterogeneous and are broadly characterized according to their activation (polarization) state by the M1/M2 classification system.⁴⁶ Some M1 and M2 markers were significantly elevated in miR-33^{-/-}Apoe^{-/-} PEMs compared with miR-33^{+/+}Apoe^{-/-} PEMs. RIP140 has been reported to promote the activity of NF-κB and to upregulate the expression of genes implicated in inflammation such as TNFα and IL-6 in macrophages.³⁸ RIP140 has been shown to be one of the targets of miR-33.³⁷ Therefore, the enhanced expression of RIP140 under miR-33 deficiency may have affected the expression of IL-6. It is also possible that elevation of M2 markers may indicate the healing process of atherosclerosis in miR-33^{-/-}Apoe^{-/-} mice and that the phenotypic changes in macrophages may involve feedback mechanisms. In any case, the effect of miR-33 deletion in macrophages is not as simple as a shift from the M1 to the M2 phenotype, as described in a previous report.¹⁹ miR-33 deficiency also

Table 2. Serum Lipid Profiling of MiR-33^{+/+}*Apoe*^{-/-} Mice Transplanted With MiR-33^{+/+}*Apoe*^{-/-} and MiR-33^{-/-}*Apoe*^{-/-} BM by Standard Method

	TC, mg/dL	HDL-C, mg/dL	LDL-C, mg/dL	TG, mg/dL
miR-33 ^{+/+} <i>Apoe</i> ^{-/-} BM recipient (n=6)	833.5±70.4	12.0±1.4	195.0±15.2	56.3±8.3
miR-33 ^{-/-} <i>Apoe</i> ^{-/-} BM recipient (n=8)	984.9±54.7	12.1±1.3	209.9±9.0	43.9±6.6
<i>P</i>	NS	NS	NS	NS

Values are mean±SE. BM indicates bone marrow; TC, total cholesterol; TG, triglyceride; LDL-C, low-density lipoprotein cholesterol; HDL-C, high-density lipoprotein cholesterol; NS, not significant.

reduced the expression of VCAM-1, which may have influenced atherosclerotic plaque formation.

We also tried to determine the contribution of the loss of miR-33 in recipient mice to atherosclerosis. However, we did not observe a significant elevation of HDL-C level in miR-33^{-/-}*Apoe*^{-/-} mice transplanted with BM of miR-33^{+/+}*Apoe*^{-/-} or miR-33^{-/-}*Apoe*^{-/-} compared with miR-33^{+/+}*Apoe*^{-/-} mice transplanted with BM of miR-33^{+/+}*Apoe*^{-/-} or miR-33^{-/-}*Apoe*^{-/-}. Currently, we do not know why HDL-C levels were almost the same in these mice. Experimental conditions such as radiation to the liver and intestine may have reduced the effect of miR-33 deficiency on the increase in HDL-C levels in recipient mice after BMT. Atherosclerotic plaque size was not significantly reduced in miR-33^{-/-}*Apoe*^{-/-} recipients compared with the miR-33^{+/+}*Apoe*^{-/-} recipients transferred with the same type of BM; this may simply indicate that the rise in HDL-C levels is important in the prevention of atherosclerosis. Our results showed that loss of miR-33 in blood cells reduced the lipid content of atherosclerotic plaque, which may be because of improved cholesterol efflux from macrophages.

A recent report indicated that the inhibition of miR-33a/b in nonhuman primates raised plasma HDL-C and lowered VLDL triglyceride levels.⁴⁷ This result was obtained from the administration of antisense miR-33 for a certain period. These

data suggest that it may be possible to inhibit miR-33a and miR-33b pharmacologically to raise HDL-C for the treatment of dyslipidemia and atherosclerosis. However, to establish the safety of this therapeutic strategy for the treatment of humans, the complete inhibition of target miRNA and longer-term assessment in animal disease models are required to avoid unexpected side effects.

Moreover, the real targets of miR-33 in vivo can only be clarified by the genetic deletion of miR-33, and the results obtained by antisense oligonucleotide-based medicine may be different from those obtained in miR-33-deficient mice. For example, the administration of miR-21 antagomir prevented pressure-overload-induced cardiac hypertrophy and fibrosis in mice⁴⁸; however, miR-21-deficient mice did not show any cardiac difference with wild-type mice under pressure overload.⁴⁹ There also seems to be a substantial difference in the effect of antisense oligonucleotide against miRNA depending on the modification such as LNA based or cholesterol modified, and many additional miRNAs that share an identical or similar sequence may be inactivated. Therefore, caution is needed when interpreting studies that use antagomir approaches to elucidate the function of individual miRNAs in vivo. Previously, we and others showed that miR-33 targets ABCA1 in macrophages and the liver. ABCG1 is another target

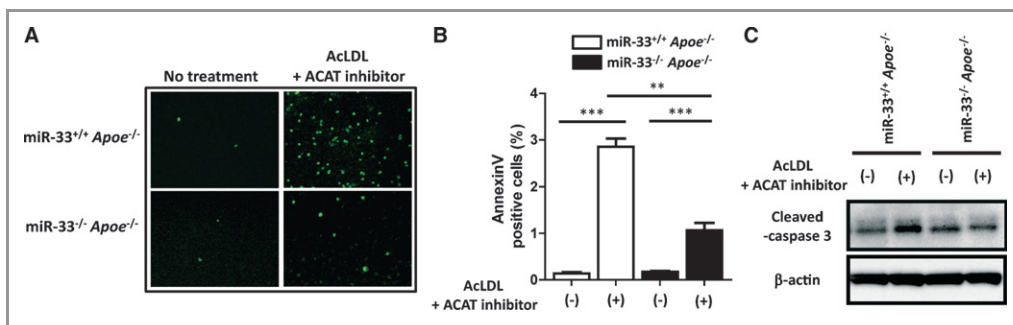


Figure 11. miR-33 deficiency ameliorated free-cholesterol loading-induced macrophage apoptosis. A, Representative microscopic images of Alexa Fluor 448-conjugated annexin V staining. Thioglycollate-elicited peritoneal macrophages from miR-33^{+/+}*Apoe*^{-/-} and miR-33^{-/-}*Apoe*^{-/-} mice were cultured in the presence or absence of acLDL plus ACAT inhibitor for 24 hours. B, Quantification of annexin V-positive macrophages in the presence or absence of acLDL plus ACAT inhibitor for 24 hours. Values are mean±SE; ***P*<0.01, ****P*<0.001. C, Western blotting analysis of cleaved caspase-3 in macrophages in the presence or absence of acLDL plus ACAT inhibitor for 48 hours. β-actin was used as a loading control.

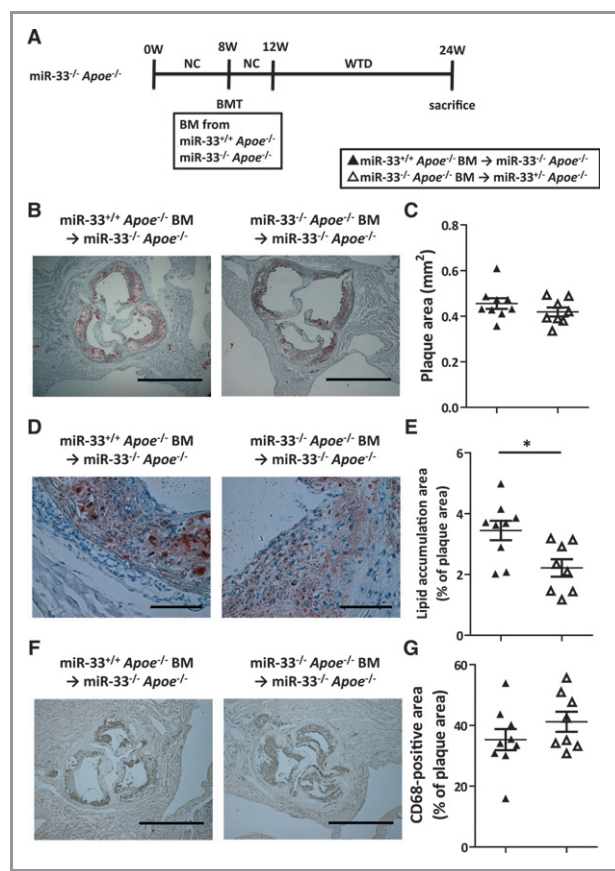


Figure 12. Lipid accumulation area in atherosclerotic lesions was reduced in miR-33^{-/-}Apoe^{-/-} mice transplanted with miR-33^{-/-}Apoe^{-/-} BM. A, Experimental protocol for bone marrow transplantation from miR-33^{+/+}Apoe^{-/-} and miR-33^{-/-}Apoe^{-/-} mice to miR-33^{-/-}Apoe^{-/-} mice. B, Representative microscopic images of cross-sections of proximal aorta in mice transplanted with miR-33^{+/+}Apoe^{-/-} and miR-33^{-/-}Apoe^{-/-} BM. Scale bar: 1 mm. C, Quantification of the atherosclerotic lesion area in cross-sections of proximal aorta. Values are mean±SE (n=8 to 9 each). D, Representative microscopic images of the lipid accumulation area in atherosclerotic lesions in mice transplanted with miR-33^{+/+}Apoe^{-/-} and miR-33^{-/-}Apoe^{-/-} BM. Scale bar: 100 μm. E, Quantification of the lipid accumulation area in cross-sections of proximal aorta. Values are mean±SE (n=8 to 9 each); *P<0.05. F, Representative microscopic images of immunohistochemical staining for the macrophage marker CD68 in mice transplanted with miR-33^{+/+}Apoe^{-/-} and miR-33^{-/-}Apoe^{-/-} BM. Scale bar: 1 mm. G, Quantification of the CD68-positive area in cross-sections of proximal aorta. Values are mean±SE (n=8 to 9 each). BM indicates bone marrow.

Table 3. Serum Lipid Profiling of MiR-33^{-/-}Apoe^{-/-} mice transplanted With MiR-33^{+/+}Apoe^{-/-} and MiR-33^{-/-}Apoe^{-/-} BM by Standard Method

	TC (mg/dL)	HDL-C (mg/dL)	LDL-C (mg/dL)	TG (mg/dL)
miR-33 ^{+/+} Apoe ^{-/-} BM recipient (n=9)	875.0±56.0	12.6±1.0	174.6±8.8	108.2±49.0
miR-33 ^{-/-} Apoe ^{-/-} BM recipient (n=5)	922.8±70.0	13.4±2.1	179.4±12.7	47.2±6.9
P	NS	NS	NS	NS

Values are mean±SE. BM indicates bone marrow; TC, total cholesterol; TG, triglyceride; LDL-C, low-density lipoprotein cholesterol; HDL-C, high-density lipoprotein cholesterol; NS, not significant.

in macrophages. In this study, we showed that ABCA1 and CROT in the livers of miR-33^{-/-}Apoe^{-/-} mice were upregulated compared with those in miR-33^{+/+}Apoe^{-/-} mice, whereas CPT1a and AMPKα were not. ABCA1, ABCG1, and RIP140 were also upregulated in miR-33^{-/-}Apoe^{-/-} macrophages. Thus, although many targets have been estimated by many computer algorithms and in vitro experiments such as luciferase-based 3' UTR analysis and Western blotting, it seems that only some of these actually have any effect in vivo through the chronic complete inhibition of miRNA.

Metabolic syndrome and type 2 diabetes are growing public health concerns worldwide that are associated with complex risk factors for cardiovascular disease (CVD). A previous meta-analysis indicated that a reduction of 2 to 3 mmol/L LDL-C by statins could reduce the risk of CVD by 40% to 50% because there was no evidence of any threshold within the cholesterol range studied.³ However, this simply means that there is still a substantial risk of CVD despite statins being widely used to lower levels of LDL-C and apolipoprotein B-containing lipoproteins. Major goals in the pursuit of novel therapeutic strategies to target this residual risk have focused on raising the amount and quality of HDL-C to prevent atherosclerosis. Further detailed experiments will be needed to determine whether targeting miR-33 could be a suitable approach for such treatment.

Acknowledgments

We thank Naoya Sowa for providing excellent technical assistance.

Sources of Funding

This work was supported in part by grants for Global COE Program “Center for Frontier Medicine” from the Ministry of Education, Culture, Sports, Science, and Technology of Japan, by grants from the Japan Society for the Promotion of Science, by a Grant-in-Aid for Scientific Research from the Ministry of Education, Culture, Sports, Science, and Technology of Japan (to T. Kimura, T. Kita, K.H., T.H., and K.O.), by a Grant-in-Aid for Scientific Research on Innovative Areas (3307) from the Ministry of Education, Culture, Sports, Science and Technology of Japan (to K.O.), by Otsuka

Pharmaceutical Co, Ltd – Kyoto University SRP Program (to T. Kimura, T. Kita, M.Y., T.H., and K.O.), by grants from Banyu Life Science Foundation International, Mochida Memorial Foundation, Kimura Memorial Heart Foundation Research Grant for 2010, Japan Heart Foundation Research Grant, Japan Heart Foundation/Novartis Grant for Research Award on Molecular and Cellular Cardiology 2011, and Takeda Memorial Foundation (to T.H.), and by grants from ONO Medical Research Foundation, The Cell Science Research Foundation, Daiichi-Sankyo Foundation of Life Science, and Takeda Memorial Foundation (to K.O.).

Disclosures

None.

References

- Baigent C, Keech A, Kearney PM, Blackwell L, Buck G, Pollicino C, Kirby A, Sourijina T, Peto R, Collins R, Simes R. Efficacy and safety of cholesterol-lowering treatment: prospective meta-analysis of data from 90,056 participants in 14 randomised trials of statins. *Lancet*. 2005;366:1267–1278.
- Kearney PM, Blackwell L, Collins R, Keech A, Simes J, Peto R, Armitage J, Baigent C. Efficacy of cholesterol-lowering therapy in 18,686 people with diabetes in 14 randomised trials of statins: a meta-analysis. *Lancet*. 2008;371:117–125.
- Baigent C, Blackwell L, Emberson J, Holland LE, Reith C, Bhalra N, Peto R, Barnes EH, Keech A, Simes J, Collins R. Efficacy and safety of more intensive lowering of LDL cholesterol: a meta-analysis of data from 170,000 participants in 26 randomised trials. *Lancet*. 2010;376:1670–1681.
- Barter P, Gotto AM, LaRosa JC, Maroni J, Szarek M, Grundy SM, Kastelein JJ, Bittner V, Fruchart JC. HDL cholesterol, very low levels of LDL cholesterol, and cardiovascular events. *N Engl J Med*. 2007;357:1301–1310.
- Wolfram RM, Brewer HB, Xue Z, Satler LF, Pichard AD, Kent KM, Waksman R. Impact of low high-density lipoproteins on in-hospital events and one-year clinical outcomes in patients with non-ST-elevation myocardial infarction acute coronary syndrome treated with drug-eluting stent implantation. *Am J Cardiol*. 2006;98:711–717.
- Gordon DJ, Probstfield JL, Garrison RJ, Neaton JD, Castelli WP, Knoke JD, Jacobs DR Jr, Bangdiwala S, Tyroler HA. High-density lipoprotein cholesterol and cardiovascular disease. Four prospective American studies. *Circulation*. 1989;79:8–15.
- Nissen SE, Tsunoda T, Tuzcu EM, Schoenhagen P, Cooper CJ, Yasin M, Eaton GM, Lauer MA, Sheldon WS, Grines CL, Halpern S, Crowe T, Blankenship JC, Kerensky R. Effect of recombinant apoA-I Milano on coronary atherosclerosis in patients with acute coronary syndromes: a randomized controlled trial. *JAMA*. 2003;290:2292–2300.
- Plump AS, Scott CJ, Breslow JL. Human apolipoprotein A-I gene expression increases high density lipoprotein and suppresses atherosclerosis in the apolipoprotein E-deficient mouse. *Proc Natl Acad Sci USA*. 1994;91:9607–9611.
- Rubin EM, Krauss RM, Spangler EA, Verstuyft JG, Clift SM. Inhibition of early atherogenesis in transgenic mice by human apolipoprotein A1. *Nature*. 1991;353:265–267.
- Aiello RJ, Brees D, Bourassa PA, Royer L, Lindsey S, Coskran T, Haghpassand M, Francone OL. Increased atherosclerosis in hyperlipidemic mice with inactivation of ABCA1 in macrophages. *Arterioscler Thromb Vasc Biol*. 2002;22:630–637.
- Joyce CW, Wagner EM, Basso F, Amar MJ, Freeman LA, Shamburek RD, Knapper CL, Syed J, Wu J, Vaisman BL, Fruchart-Najib J, Billings EM, Paigen B, Remaley AT, Santamarina-Fojo S, Brewer HB Jr. ABCA1 overexpression in the liver of LDLr-KO mice leads to accumulation of pro-atherogenic lipoproteins and enhanced atherosclerosis. *J Biol Chem*. 2006;281:33053–33065.
- Singaraja RR, Fievet C, Castro G, James ER, Hennuyer N, Clee SM, Bissada N, Choy JC, Fruchart JC, McManus BM, Staels B, Hayden MR. Increased ABCA1 activity protects against atherosclerosis. *J Clin Invest*. 2002;110:35–42.
- van Eck M, Bos IS, Kaminski WE, Orso E, Rothe G, Twisk J, Botcher A, Van Amersfoort ES, Christiansen-Weber TA, Fung-Leung WP, Van Berkel TJ, Schmitz G. Leukocyte ABCA1 controls susceptibility to atherosclerosis and macrophage recruitment into tissues. *Proc Natl Acad Sci USA*. 2002;99:6298–6303.
- Brunham LR, Singaraja RR, Duong M, Timmins JM, Fievet C, Bissada N, Kang MH, Samra A, Fruchart JC, McManus B, Staels B, Parks JS, Hayden MR. Tissue-specific roles of ABCA1 influence susceptibility to atherosclerosis. *Arterioscler Thromb Vasc Biol*. 2009;29:548–554.
- Tang C, Liu Y, Kessler PS, Vaughan AM, Oram JF. The macrophage cholesterol exporter ABCA1 functions as an anti-inflammatory receptor. *J Biol Chem*. 2009;284:32336–32343.
- Rayner KJ, Suarez Y, Davalos A, Parathath S, Fitzgerald ML, Tamehiro N, Fisher EA, Moore KJ, Fernandez-Hernando C. MiR-33 contributes to the regulation of cholesterol homeostasis. *Science*. 2010;328:1570–1573.
- Najafi-Shoushtari SH, Kristo F, Li Y, Shioda T, Cohen DE, Gerszten RE, Naar AM. MicroRNA-33 and the SREBP host genes cooperate to control cholesterol homeostasis. *Science*. 2010;328:1566–1569.
- Marquart TJ, Allen RM, Ory DS, Baldan A. MiR-33 links SREBP-2 induction to repression of sterol transporters. *Proc Natl Acad Sci USA*. 2010;107:12228–12232.
- Rayner KJ, Sheedy FJ, Esau CC, Hussain FN, Temel RE, Parathath S, van Gils JM, Rayner AJ, Chang AN, Suarez Y, Fernandez-Hernando C, Fisher EA, Moore KJ. Antagonism of miR-33 in mice promotes reverse cholesterol transport and regression of atherosclerosis. *J Clin Invest*. 2011;121:2921–2931.
- Plump AS, Smith JD, Hayek T, Aalto-Setälä K, Walsh A, Verstuyft JG, Rubin EM, Breslow JL. Severe hypercholesterolemia and atherosclerosis in apolipoprotein E-deficient mice created by homologous recombination in ES cells. *Cell*. 1992;71:343–353.
- Zhang SH, Reddick RL, Piedrahita JA, Maeda N. Spontaneous hypercholesterolemia and arterial lesions in mice lacking apolipoprotein E. *Science*. 1992;258:468–471.
- Horie T, Ono K, Horiguchi M, Nishi H, Nakamura T, Nagao K, Kinoshita M, Kuwabara Y, Marusawa H, Iwanaga Y, Hasegawa K, Yokode M, Kimura T, Kita T. MicroRNA-33 encoded by an intron of sterol regulatory element-binding protein 2 (SREBP2) regulates HDL in vivo. *Proc Natl Acad Sci USA*. 2010;107:17321–17326.
- Horie T, Ono K, Nishi H, Nagao K, Kinoshita M, Watanabe S, Kuwabara Y, Nakashima Y, Takanabe-Mori R, Nishi E, Hasegawa K, Kita T, Kimura T. Acute doxorubicin cardiotoxicity is associated with miR-146A-induced inhibition of the neuregulin-ERBB pathway. *Cardiovasc Res*. 2010;87:656–664.
- de la Llera-Moya M, Drazul-Schrader D, Asztalos BF, Cuchel M, Rader DJ, Rothblat GH. The ability to promote efflux via ABCA1 determines the capacity of serum specimens with similar high-density lipoprotein cholesterol to remove cholesterol from macrophages. *Arterioscler Thromb Vasc Biol*. 2010;30:796–801.
- Khera AV, Cuchel M, de la Llera-Moya M, Rodrigues A, Burke MF, Jafri K, French BC, Phillips JA, Mucksavage ML, Wilensky RL, Mohler ER, Rothblat GH, Rader DJ. Cholesterol efflux capacity, high-density lipoprotein function, and atherosclerosis. *N Engl J Med*. 2011;364:127–135.
- Asztalos BF, de la Llera-Moya M, Dallal GE, Horvath KV, Schaefer EJ, Rothblat GH. Differential effects of HDL subpopulations on cellular ABCA1- and SR-BI-mediated cholesterol efflux. *J Lipid Res*. 2005;46:2246–2253.
- Yvan-Charvet L, Ranalletta M, Wang N, Han S, Terasaka N, Li R, Welch C, Tall AR. Combined deficiency of ABCA1 and ABCG1 promotes foam cell accumulation and accelerates atherosclerosis in mice. *J Clin Invest*. 2007;117:3900–3908.
- Van Eck M, Singaraja RR, Ye D, Hildebrand RB, James ER, Hayden MR, Van Berkel TJ. Macrophage ATP-binding cassette transporter A1 overexpression inhibits atherosclerotic lesion progression in low-density lipoprotein receptor knockout mice. *Arterioscler Thromb Vasc Biol*. 2006;26:929–934.
- Aparicio-Vergara M, Shiri-Sverdlov R, de Haan G, Hofker MH. Bone marrow transplantation in mice as a tool for studying the role of hematopoietic cells in metabolic and cardiovascular diseases. *Atherosclerosis*. 2010;213:335–344.
- Paigen B, Morrow A, Holmes PA, Mitchell D, Williams RA. Quantitative assessment of atherosclerotic lesions in mice. *Atherosclerosis*. 1987;68:231–240.
- Tangirala RK, Rubin EM, Palinski W. Quantitation of atherosclerosis in murine models: correlation between lesions in the aortic origin and in the entire aorta, and differences in the extent of lesions between sexes in LDL receptor-deficient and apolipoprotein E-deficient mice. *J Lipid Res*. 1995;36:2320–2328.
- Kobayashi T, Tahara Y, Matsumoto M, Iguchi M, Sano H, Murayama T, Arai H, Oida H, Yurugi-Kobayashi T, Yamashita JK, Katagiri H, Majima M, Yokode M, Kita T, Narumiya S. Roles of thromboxane A(2) and prostacyclin in the development of atherosclerosis in apoE-deficient mice. *J Clin Invest*. 2004;114:784–794.

33. Yao PM, Tabas I. Free cholesterol loading of macrophages is associated with widespread mitochondrial dysfunction and activation of the mitochondrial apoptosis pathway. *J Biol Chem*. 2001;276:42468–42476.
34. Devries-Seimon T, Li Y, Yao PM, Stone E, Wang Y, Davis RJ, Flavell R, Tabas I. Cholesterol-induced macrophage apoptosis requires ER stress pathways and engagement of the type A scavenger receptor. *J Cell Biol*. 2005;171:61–73.
35. Folch J, Lees M, Sloane Stanley GH. A simple method for the isolation and purification of total lipides from animal tissues. *J Biol Chem*. 1957;226:497–509.
36. Tacke F, Alvarez D, Kaplan TJ, Jakubzick C, Spanbroek R, Llodra J, Garin A, Liu J, Mack M, van Rooijen N, Lira SA, Habenicht AJ, Randolph GJ. Monocyte subsets differentially employ CCR2, CCR5, and CX3CR1 to accumulate within atherosclerotic plaques. *J Clin Invest*. 2007;117:185–194.
37. Ho PC, Chang KC, Chuang YS, Wei LN. Cholesterol regulation of receptor-interacting protein 140 via microRNA-33 in inflammatory cytokine production. *Faseb J*. 2011;25:1758–1766.
38. Fritah A, Christian M, Parker MG. The metabolic coregulator RIP140: an update. *Am J Physiol Endocrinol Metab*. 2010;299:E335–340.
39. Timmins JM, Lee JY, Boudyguina E, Kluckman KD, Brunham LR, Mulya A, Gebre AK, Coutinho JM, Colvin PL, Smith TL, Hayden MR, Maeda N, Parks JS. Targeted inactivation of hepatic ABCA1 causes profound hypoalphalipoproteinemia and kidney hypercatabolism of apoA-I. *J Clin Invest*. 2005;115:1333–1342.
40. Brunham LR, Kruit JK, Pape TD, Parks JS, Kuipers F, Hayden MR. Tissue-specific induction of intestinal ABCA1 expression with a liver × receptor agonist raises plasma HDL cholesterol levels. *Circ Res*. 2006;99:672–674.
41. Scull CM, Tabas I. Mechanisms of ER stress-induced apoptosis in atherosclerosis. *Arterioscler Thromb Vasc Biol*. 2011;31:2792–2797.
42. Thorp E, Li G, Seimon TA, Kuriakose G, Ron D, Tabas I. Reduced apoptosis and plaque necrosis in advanced atherosclerotic lesions of apoE^{-/-} and LDLR^{-/-} mice lacking chop. *Cell Metab*. 2009;9:474–481.
43. Seimon TA, Nadolski MJ, Liao X, Magallon J, Nguyen M, Feric NT, Koschinsky ML, Harkewicz R, Witztum JL, Tsimikas S, Golenbock D, Moore KJ, Tabas I. Atherogenic lipids and lipoproteins trigger CD36-TLR2-dependent apoptosis in macrophages undergoing endoplasmic reticulum stress. *Cell Metab*. 2010;12:467–482.
44. Yvan-Charvet L, Pagler T, Gautier EL, Avagyan S, Siry RL, Han S, Welch CL, Wang N, Randolph GJ, Snoeck HW, Tall AR. ATP-binding cassette transporters and HDL suppress hematopoietic stem cell proliferation. *Science*. 2010;328:1689–1693.
45. Collier BS. Leukocytosis and ischemic vascular disease morbidity and mortality: is it time to intervene? *Arterioscler Thromb Vasc Biol*. 2005;25:658–670.
46. Martinez FO, Helming L, Gordon S. Alternative activation of macrophages: an immunologic functional perspective. *Annu Rev Immunol*. 2009;27:451–483.
47. Rayner KJ, Esau CC, Hussain FN, McDaniel AL, Marshall SM, van Gils JM, Ray TD, Sheedy FJ, Goedeke L, Liu X, Khatsenko OG, Kaimal V, Lees CJ, Fernandez-Hernando C, Fisher EA, Temel RE, Moore KJ. Inhibition of miR-33a/b in non-human primates raises plasma HDL and lowers VLDL triglycerides. *Nature*. 2011;478:404–407.
48. Thum T, Gross C, Fiedler J, Fischer T, Kissler S, Bussen M, Galuppo P, Just S, Rottbauer W, Frantz S, Castoldi M, Soutschek J, Koteliensky V, Rosenwald A, Basson MA, Licht JD, Pena JT, Rouhanifard SH, Muckenthaler MU, Tuschl T, Martin GR, Bauersachs J, Engelhardt S. MicroRNA-21 contributes to myocardial disease by stimulating map kinase signalling in fibroblasts. *Nature*. 2008;456:980–984.
49. Patrick DM, Montgomery RL, Qi X, Obad S, Kauppinen S, Hill JA, van Rooij E, Olson EN. Stress-dependent cardiac remodeling occurs in the absence of microRNA-21 in mice. *J Clin Invest*. 2010;120:3912–3916.